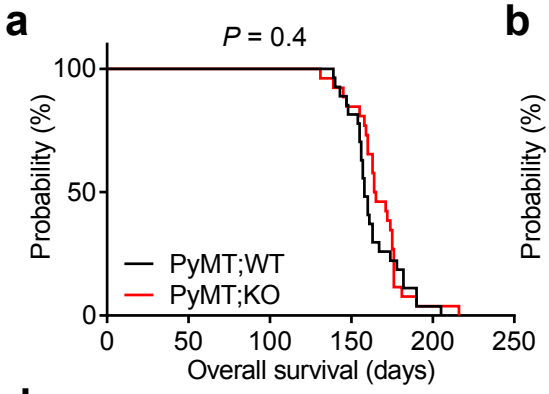

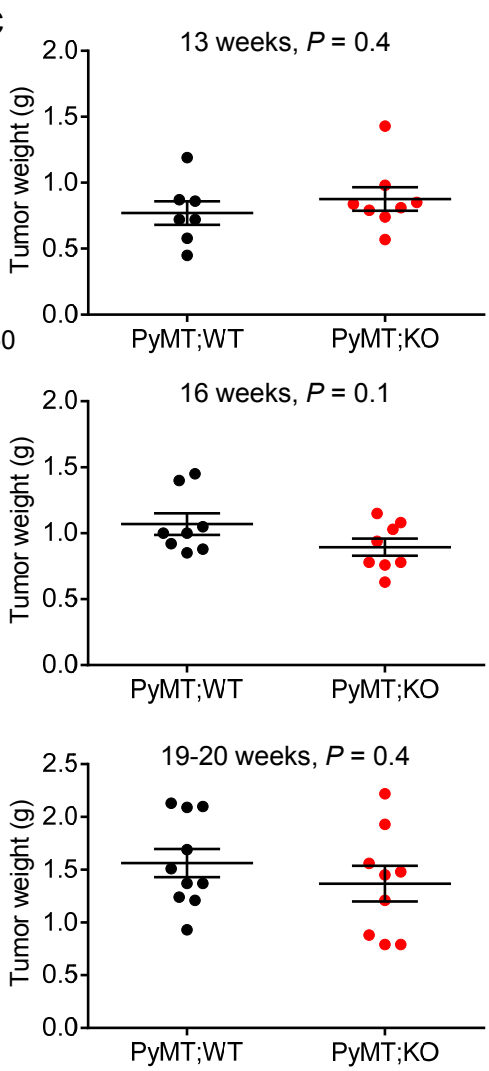

d

PyMT;	WT-13w	KO-13w	WT-16w	KO-16w	WT-19w	KO-19w
Normal	0	0	0	0	0	0
Focal Hyperplasia	4	4	0	0	0	0
Hyperplasia	0	3	0	2	0	0
Very small foci of breast AdCa	0	0	0	0	0	0
Small foci of breast AdCa	9	9	10	12	0	3
Breast AdCa	3	0	6	2	10	7
n =	16	16	16	16	10	10
P value:		0.3		0.05		0.08

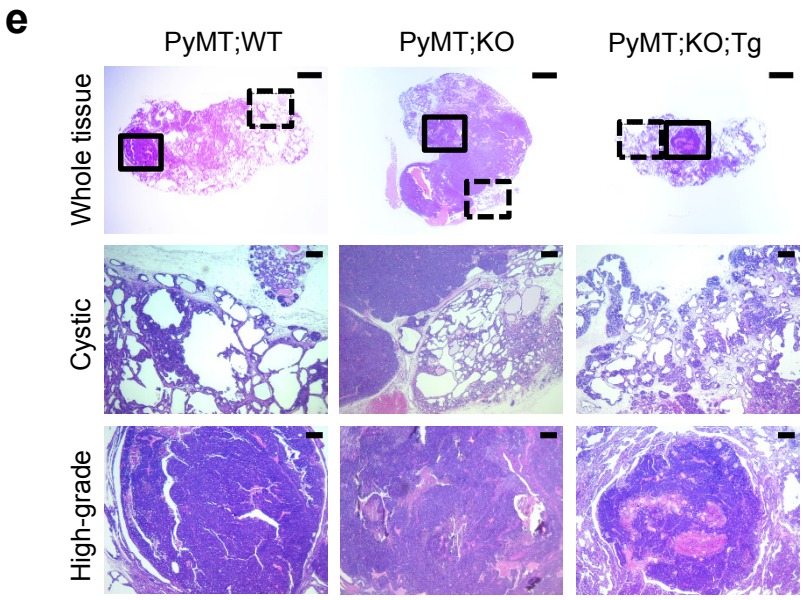

Supplementary Figure 1

Insertional inactivation of *Malat1* in mice does not affect mammary tumor onset, growth, or histology.

(**a, b**) Overall survival (**a**, *n* = 27 and 26 mice per group) and mammary tumor-free survival (**b**, determined by palpation performed three times a week, *n* = 17 mice per group) of MMTV-PyMT;*Malat1*$^{+/+}$ (PyMT;WT) and MMTV-PyMT;*Malat1*$^{-/-}$ (PyMT;KO) mice. Mice were euthanized when they met the institutional euthanasia criteria for tumor size (2 cm in diameter). Statistical significance was determined by a log-rank test. (**c**) Weight of the mammary tumors of PyMT;WT and PyMT;KO mice at 13 (*n* = 7 and 8 mice per group), 16 (*n* = 8 mice per group), and 19-20 (*n* = 10 and 9 mice per group) weeks of age. (**d**) Histopathological examination of the mammary tissues of PyMT;WT and PyMT;KO mice at 13, 16, and 19-20 weeks of age. AdCa: adenocarcinoma. (**e**) H&E staining of the mammary tumors of PyMT;WT, PyMT;KO, and PyMT;KO;Tg mice. In upper panels, boxed areas with dashed and solid lines indicate cystic and high-grade carcinoma regions, respectively. Images are representative of three random fields per group. Scale bars, 2 mm in upper panels and 200 μm in middle and lower panels. Statistical significance was determined by an unpaired *t*-test in (**c**) and (**d**). Error bars are s.e.m. Mouse strain: B6.

Supplementary Figure 2

a

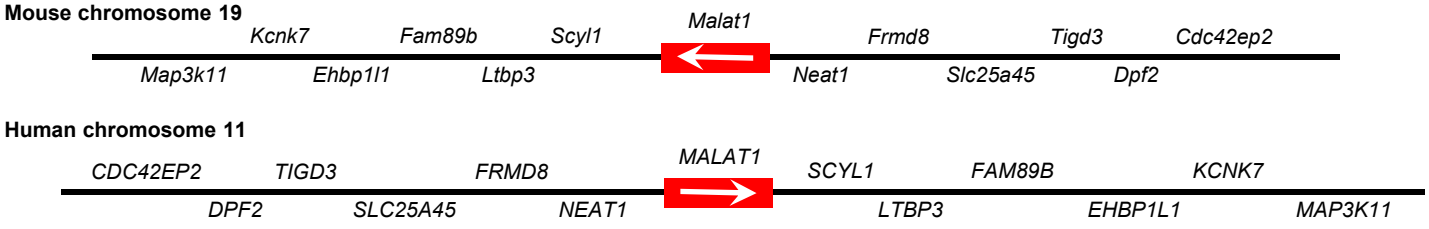

b

Gene	logFC	K/W	% change in KO	*P* value
Frmd8	0.112	1.081	+8.070	0.042
Tigd3	0.021	1.015	+1.461	0.287
Ltbp3	0.040	1.028	+2.780	0.123
Ehbp1l1	0.025	1.017	+1.744	0.216
Cdc42ep2	0.035	1.025	+2.458	0.131
Dpf2	0.023	1.016	+1.638	0.190
Slc25a45	0.023	1.016	+1.599	0.131
Scyl1	0.041	1.029	+2.889	0.042
Kcnk7	0.028	1.020	+1.986	0.019
Map3k11	0.015	1.010	+1.043	0.413
Fam89b	N/A	N/A	N/A	N/A
Neat1	N/A	N/A	N/A	N/A

c

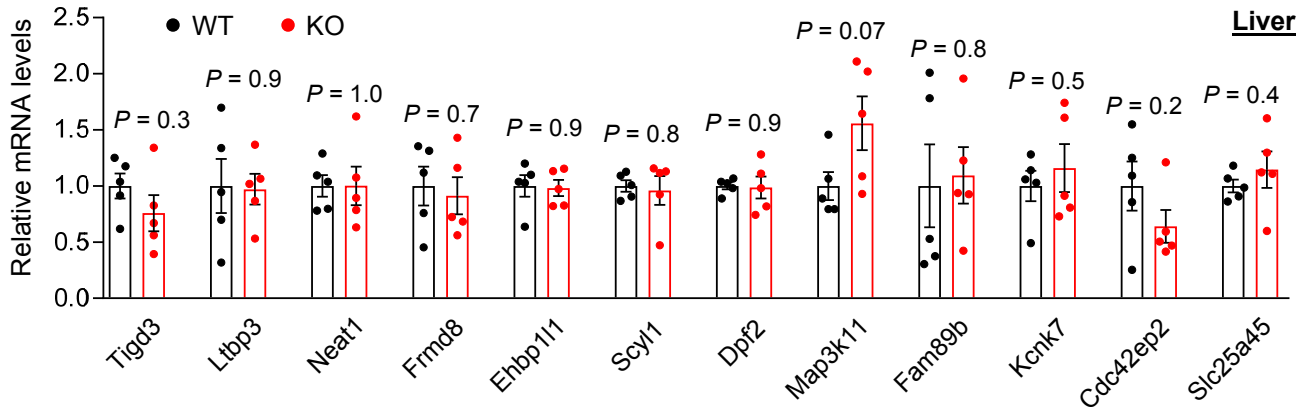

d

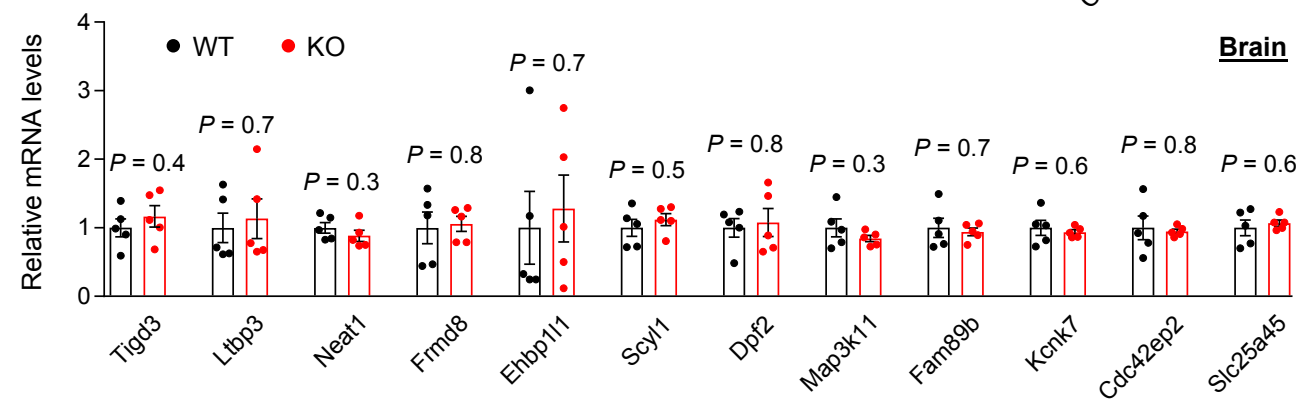

e

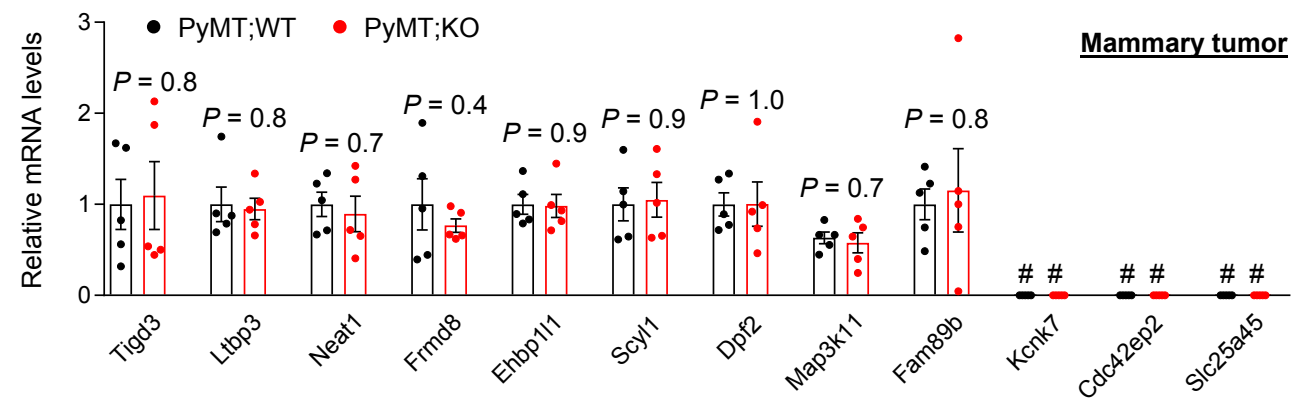

Supplementary Figure 2

Insertional inactivation of *Malat1* in mice does not affect *Malat1*'s adjacent gene expression.

(**a**) Schematic diagram (not drawn to scale) of the genomic loci of mouse and human *MALAT1* and the 12 adjacent genes. (**b**) Microarray data from Nakagawa *et al*., 2012 (accession number GSE37707, see URLs) comparing 12 *Malat1*'s adjacent gene expression levels in *Malat1* wild-type (W) and *Malat1* knockout (K) hippocampus. *Fam89b* and *Neat1* were not available in the original microarray dataset. *n* = 2 mice per group. (**c, d**) qPCR of 12 *Malat1*'s adjacent genes (*Tigd3*, *Ltbp3*, *Neat1*, *Frmd8*, *Ehbp1l1, Scyl1, Dpf2, Map3k11, Fam89b, Kcnk7, Cdc42ep2*, and *Slc25a45*) in the liver (**c**) and brain (**d**) tissues of $Malat1^{+/+}$ (WT) and $Malat1^{-/-}$ (KO) mice. *n* = 5 mice per group. Results are representative of two independent experiments. (**e**) qPCR of 12 *Malat1*'s adjacent genes (*Tigd3*, *Ltbp3*, *Neat1*, *Frmd8*, *Ehbp1l1, Scyl1, Dpf2, Map3k11, Fam89b, Kcnk7, Cdc42ep2*, and *Slc25a45*) in the mammary tumors of MMTV-PyMT;$Malat1^{+/+}$ (PyMT;WT) and MMTV-PyMT;$Malat1^{-/-}$ (PyMT;KO) mice. #: not detectable. *n* = 5 mice per group. Results are representative of two independent experiments. Statistical significance was determined by an unpaired *t*-test in (**b**)-(**e**). Error bars are s.e.m. Mouse strain: B6.

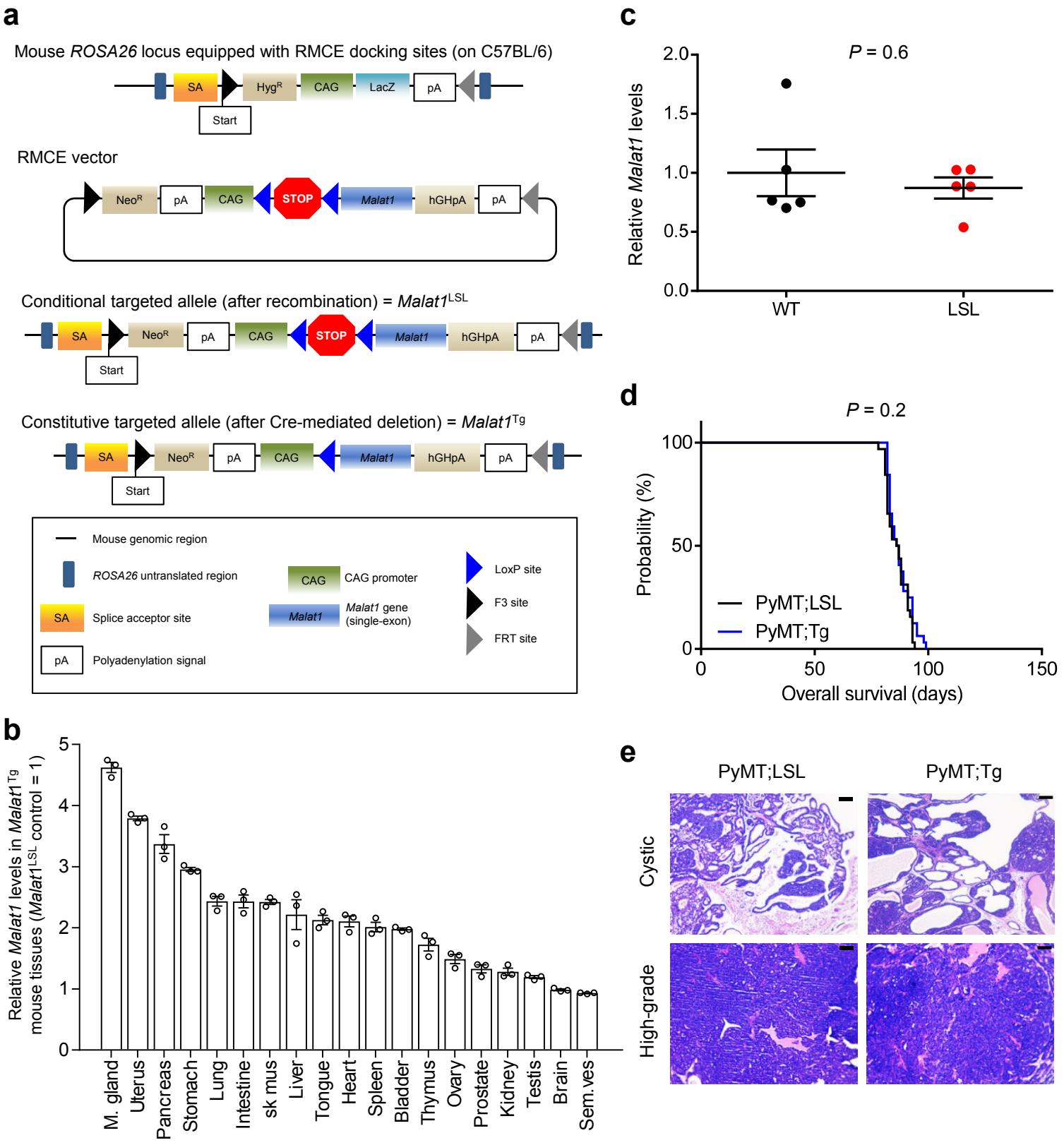
a
Mouse ROSA26 locus equipped with RMCE docking sites (on C57BL/6)
SA
Hygʳ
CAG
LacZ
pA
Start
RMCE vector
Neoʳ
pA
CAG
STOP
Malat1
hGHpA
pA
Conditional targeted allele (after recombination) = Malat1LSL
Constitutive targeted allele (after Cre-mediated deletion) = Malat1Tg
Mouse genomic region
ROSA26 untranslated region
Splice acceptor site
Polyadenylation signal
CAG promoter
Malat1 gene (single-exon)
LoxP site
F3 site
FRT site
b
Relative Malat1 levels in Malat1Tg mouse tissues (Malat1LSL control = 1)
M. gland
Uterus
Pancreas
Stomach
Lung
Intestine
sk mus
Liver
Tongue
Heart
Spleen
Bladder
Thymus
Ovary
Prostate
Kidney
Testis
Brain
Sem.ves
c
P = 0.6
Relative Malat1 levels
WT
LSL
d
P = 0.2
Probability (%)
PyMT;LSL
PyMT;Tg
Overall survival (days)
e
PyMT;LSL
PyMT;Tg
Cystic
High-grade

Supplementary Figure 3

Targeted transgenic overexpression of *Malat1* in mice does not affect survival or primary mammary tumors.

(**a**) The strategy used to generate mice with targeted transgenic overexpression of *Malat1* from the *ROSA26* locus (on a B6 background). LSL, LoxP-STOP-LoxP; Tg, transgenic. (**b**) qPCR of *Malat1* in multiple tissues of *Malat1*^{Tg} mice. Data are normalized to the *Malat1*^{LSL} control mice. Error bars are s.e.m. of three technical replicates per tissue and results are representative of two independent experiments. M. gland = mammary gland; sk mus = skeletal muscle; sem. ves = seminal vesicle. (**c**) qPCR of *Malat1* in the mammary tissues of non-targeted wild-type and *Malat1*^{LSL} mice. Statistical significance was determined by an unpaired *t*-test. Error bars are s.e.m. *n* = 5 mice per group. Results are representative of two independent experiments. (**d**) Overall survival of MMTV-PyMT;*Malat1*^{LSL} (PyMT;LSL) and MMTV-PyMT;*Malat1*^{Tg} (PyMT;Tg) mice. Mice were euthanized when they met the institutional euthanasia criteria for primary tumor size (2 cm in diameter). Statistical significance was determined by a log-rank test. *n* = 32 mice per group. (**e**) H&E staining of the mammary tumors of PyMT;LSL and PyMT;Tg mice. Upper and lower panels show cystic and high-grade carcinoma regions, respectively. Images are representative of three random fields per group. Scale bars, 100 μm. Mouse strains: B6 in (**b**) and (**c**); FVB in (**d**) and (**e**).

Supplementary Figure 4

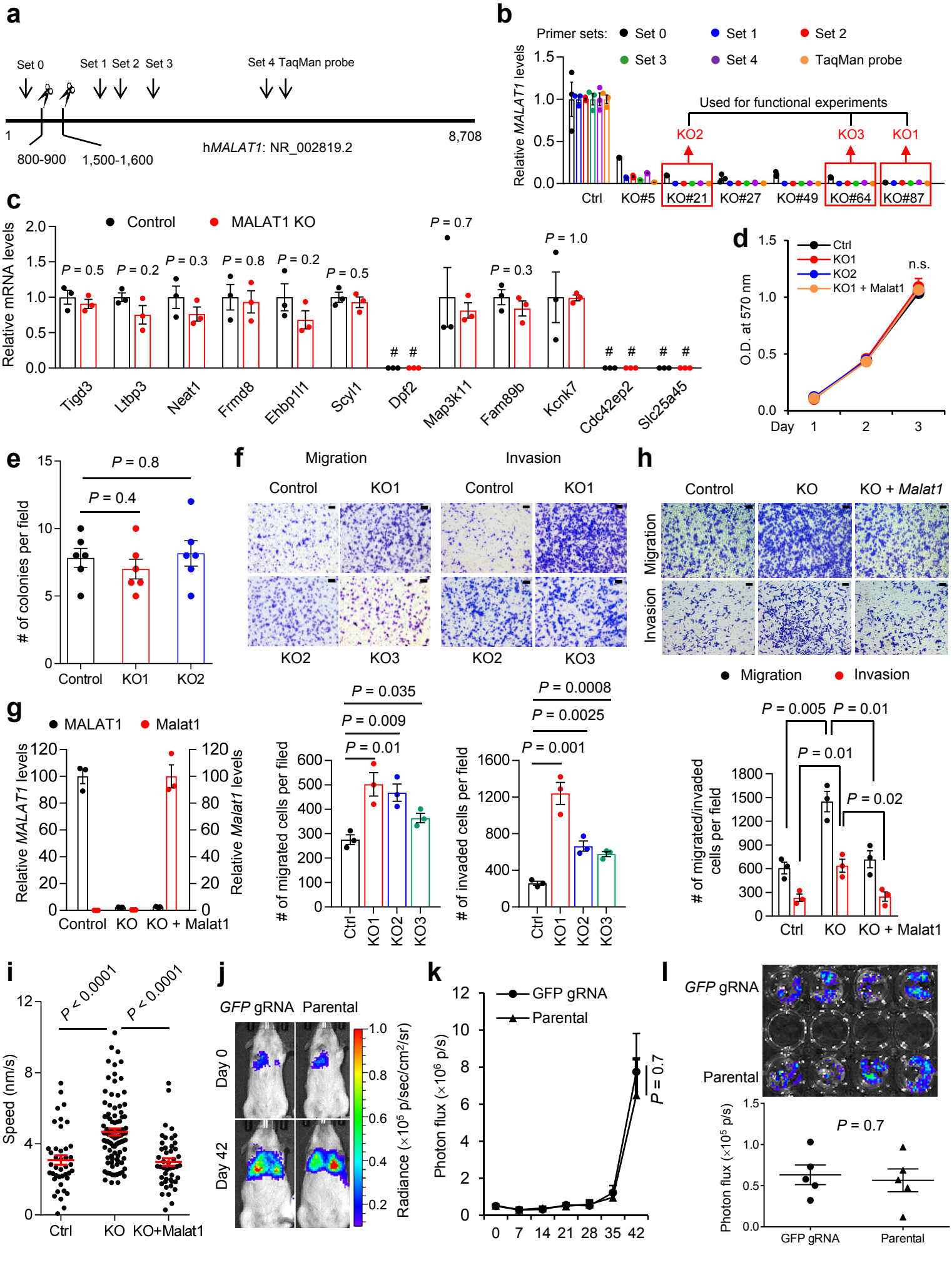

Supplementary Figure 4

Loss of *MALAT1* promotes metastatic ability of human breast cancer cells.

(**a**) Location of each primer set and the TaqMan probe on human *MALAT1*, which were used for RT-qPCR in **Supplementary Fig. 4b**. (**b**) qPCR of *MALAT1* in six *MALAT1* knockout clones of MDA-MB-231 cells generated by DECKO. Cells expressing *GFP* gRNA were used as the control (Ctrl). *n* = 3 technical replicates per cell line. Results are representative of two independent experiments. (**c**) qPCR of 12 *MALAT1*'s adjacent genes (*TIGD3*, *LTBP3*, *NEAT1*, *FRMD8*, *EHBP1L1, SCYL1, DPF2, MAP3K11, FAM89B, KCNK7, CDC42EP2*, and *SLC25A45*) in control and *MALAT1* knockout (KO1) MDA-MB-231 cells. #: not detectable. *n* = 3 technical replicates per group. Results are representative of two independent experiments. (**d**) Growth curves of control, *MALAT1* knockout, and *Malat1*-restored MDA-MB-231 cells. *n* = 4 cell culture replicates per group. Results are representative of three independent experiments. n.s.: not significant ($P \geq 0.05$). (**e**) Anchorage-independent growth (soft agar colony formation) of two *MALAT1* knockout clones of MDA-MB-231 cells. *n* = 6 cell culture replicates per group. Results are representative of two independent experiments. (**f**) Images (upper panel) and data quantification (lower panel) of migration and invasion assays of three *MALAT1* knockout clones of MDA-MB-231 cells. *n* = 3 cell culture replicates per group. Results are representative of three independent experiments and images are representative of three random fields per group. Scale bars, 100 μm. (**g**) qPCR of human *MALAT1* and mouse *Malat1* in control, *MALAT1* knockout, and *Malat1*-restored MDA-MB-231 cells. *n* = 3 technical replicates per group. Results are representative of three independent experiments. (**h**) Images (upper panel) and data quantification (lower panel) of migration and invasion assays of control, *MALAT1* knockout, and *Malat1*-restored MDA-MB-231 cells. *n* = 3 cell culture replicates per group. Results are representative of two independent experiments and images are representative of three random fields per group. Scale bars, 100 μm. (**i**) Quantification of the speed of movement (nm/sec) of control, *MALAT1* knockout, and *Malat1*-restored MDA-MB-231 cells. *n* = 41, 93, and 46 randomly and automatically generated tracks per group, respectively. Results are representative of three independent experiments. (**j, k**) Bioluminescent imaging (**j**) and quantification of photon flux (**k**) of live NSG mice with tail vein injection of luciferase-labeled parental MDA-MB-231 cells or MDA-MB-231 cells expressing the *GFP* gRNA. *n* = 5 mice per group. (**l**) *Ex vivo* bioluminescent imaging (upper panel) and quantification of photon flux (lower panel) of the lungs dissected from NSG mice with tail vein injection of luciferase-labeled parental MDA-MB-231 cells or MDA-MB-231 cells expressing the *GFP* gRNA. *n* = 5 mice per group. Statistical significance in (**c**)-(**f**) and (**h**), (**i**), (**k**), and (**l**) was determined by an unpaired *t*-test. Error bars are s.e.m.

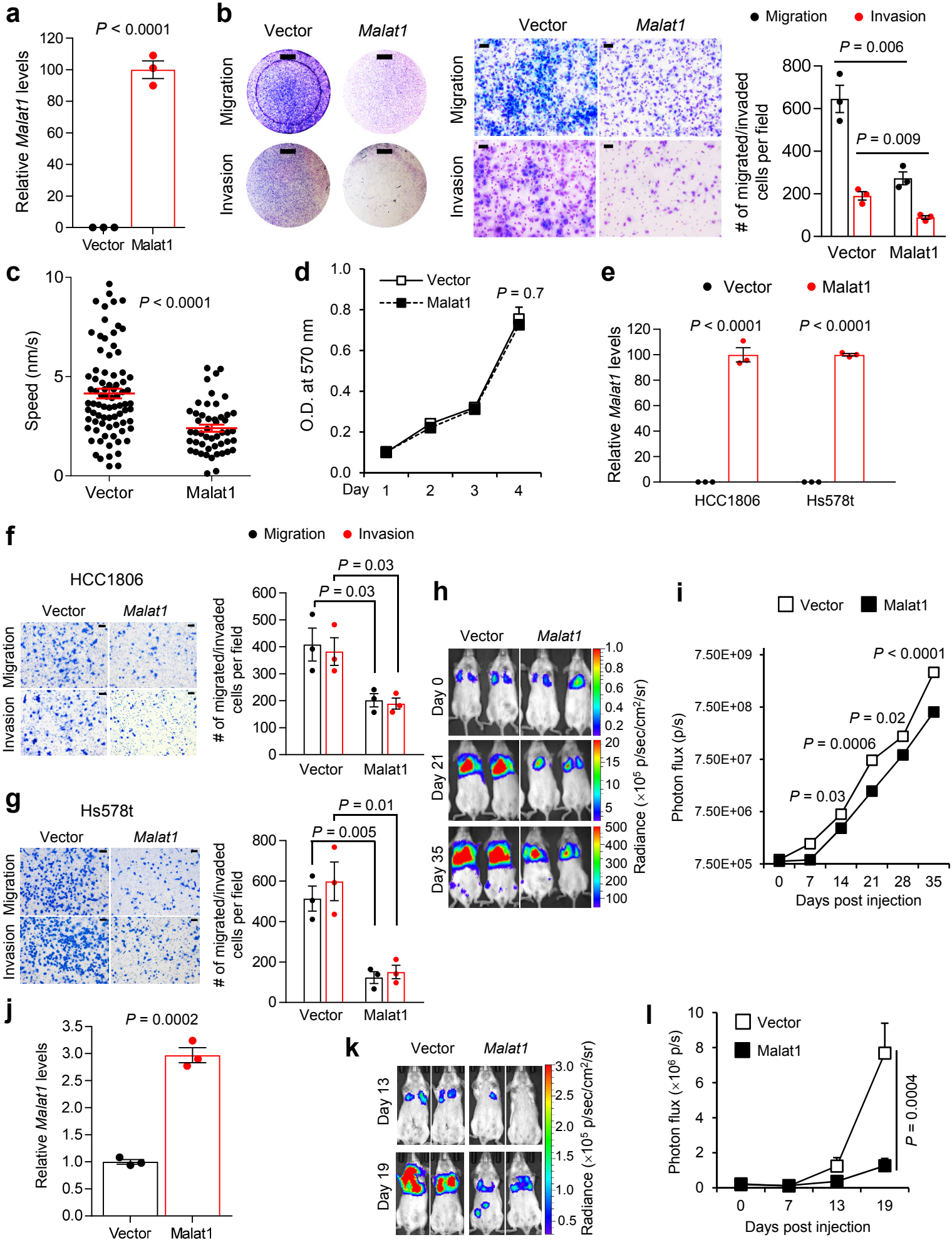
a
P < 0.0001
Relative Malat1 levels
120
100
80
60
40
20
0
Vector
Malat1
b
Vector
Malat1
Migration
Invasion
Vector
Malat1
Migration
Invasion
Migration
Invasion
P = 0.006
P = 0.009
# of migrated/invaded cells per field
800
600
400
200
0
Vector
Malat1
c
P < 0.0001
Speed (nm/s)
10
5
0
Vector
Malat1
d
Vector
Malat1
P = 0.7
O.D. at 570 nm
1.0
0.8
0.6
0.4
0.2
0.0
Day 1 2 3 4
e
Vector
Malat1
P < 0.0001
P < 0.0001
Relative Malat1 levels
120
100
80
60
40
20
0
HCC1806
Hs578t
f
Migration
Invasion
HCC1806
Vector
Malat1
Migration
Invasion
P = 0.03
P = 0.03
# of migrated/invaded cells per field
600
500
400
300
200
100
0
Vector
Malat1
g
Hs578t
Vector
Malat1
Migration
Invasion
P = 0.01
P = 0.005
# of migrated/invaded cells per field
800
600
400
200
0
Vector
Malat1
h
Vector
Malat1
Day 0
Day 21
Day 35
1.0
0.8
0.6
0.4
0.2
20
15
10
5
500
400
300
200
100
Radiance (×10⁵ p/sec/cm²/sr)
i
Vector
Malat1
P < 0.0001
P = 0.02
P = 0.0006
P = 0.03
Photon flux (p/s)
7.50E+09
7.50E+08
7.50E+07
7.50E+06
7.50E+05
0 7 14 21 28 35
Days post injection
j
P = 0.0002
Relative Malat1 levels
3.5
3.0
2.5
2.0
1.5
1.0
0.5
0.0
Vector
Malat1
k
Vector
Malat1
Day 13
Day 19
3.0
2.5
2.0
1.5
1.0
0.5
Radiance (×10⁵ p/sec/cm²/sr)
l
Vector
Malat1
P = 0.0004
Photon flux (×10⁶ p/s)
10
8
6
4
2
0
0 7 13 19
Days post injection

Supplementary Figure 5

Gain of *Malat1* inhibits metastatic ability of human and mouse breast cancer cells.

(**a**) qPCR of *Malat1* in LM2 cells stably transfected with mouse *Malat1*. *n* = 3 technical replicates per group. Results are representative of four independent experiments. (**b**) Images (left panel) and data quantification (right panel) of migration and invasion assays of LM2 cells stably transfected with mouse *Malat1*. *n* = 3 cell culture replicates per group. Results are representative of three independent experiments. Low-power images (left panel) are representative whole-membranes of three cell culture replicates per group and high-power images (right panel) are representative of four random fields per group. Scale bars, 2 mm (low magnification) and 50 μm (high magnification). (**c**) Quantification of the speed of movement (nm/sec) of LM2 cells stably transfected with mouse *Malat1*. *n* = 80 and 49 randomly and automatically generated tracks per group, respectively. Results are representative of two independent experiments. (**d**) Growth curves of LM2 cells stably transfected with mouse *Malat1*. *n* = 4 cell culture replicates per group. Results are representative of four independent experiments. (**e**) qPCR of *Malat1* in HCC1806 and Hs578t cells transfected with mouse *Malat1*. *n* = 3 technical replicates per group. Results are representative of two independent experiments. (**f, g**) Images (left panel) and data quantification (right panel) of migration and invasion assays of HCC1806 (**f**) and Hs578t (**g**) cells transfected with mouse *Malat1*. *n* = 3 cell culture replicates per group. Results are representative of two independent experiments and images are representative of three random fields per group. Scale bars, 100 μm. (**h, i**) Bioluminescent imaging (**h**) and quantification of photon flux (**i**, presented on a log10 scale) of live NSG mice with tail vein injection of control (*n* = 9 mice) or *Malat1*-overexpressing (*n* = 10 mice) LM2 cells, at different time points. Day 0: the day of tumor cell injection. (**j**) qPCR of *Malat1* in control and *Malat1*-overexpressing 4T1 cells. *n* = 3 technical replicates per group. Results are representative of three independent experiments. (**k, l**) Bioluminescent imaging (**k**) and quantification of photon flux (**l**) of live BALB/c mice with tail vein injection of control or *Malat1*-overexpressing 4T1 cells, at different time points. *n* = 9 and 10 mice were injected with control and *Malat1*-overexpressing 4T1 cells, respectively. Statistical significance in (**a**)-(**g**), (**i**), (**j**), and (**l**) was determined by an unpaired *t*-test. Error bars are s.e.m.

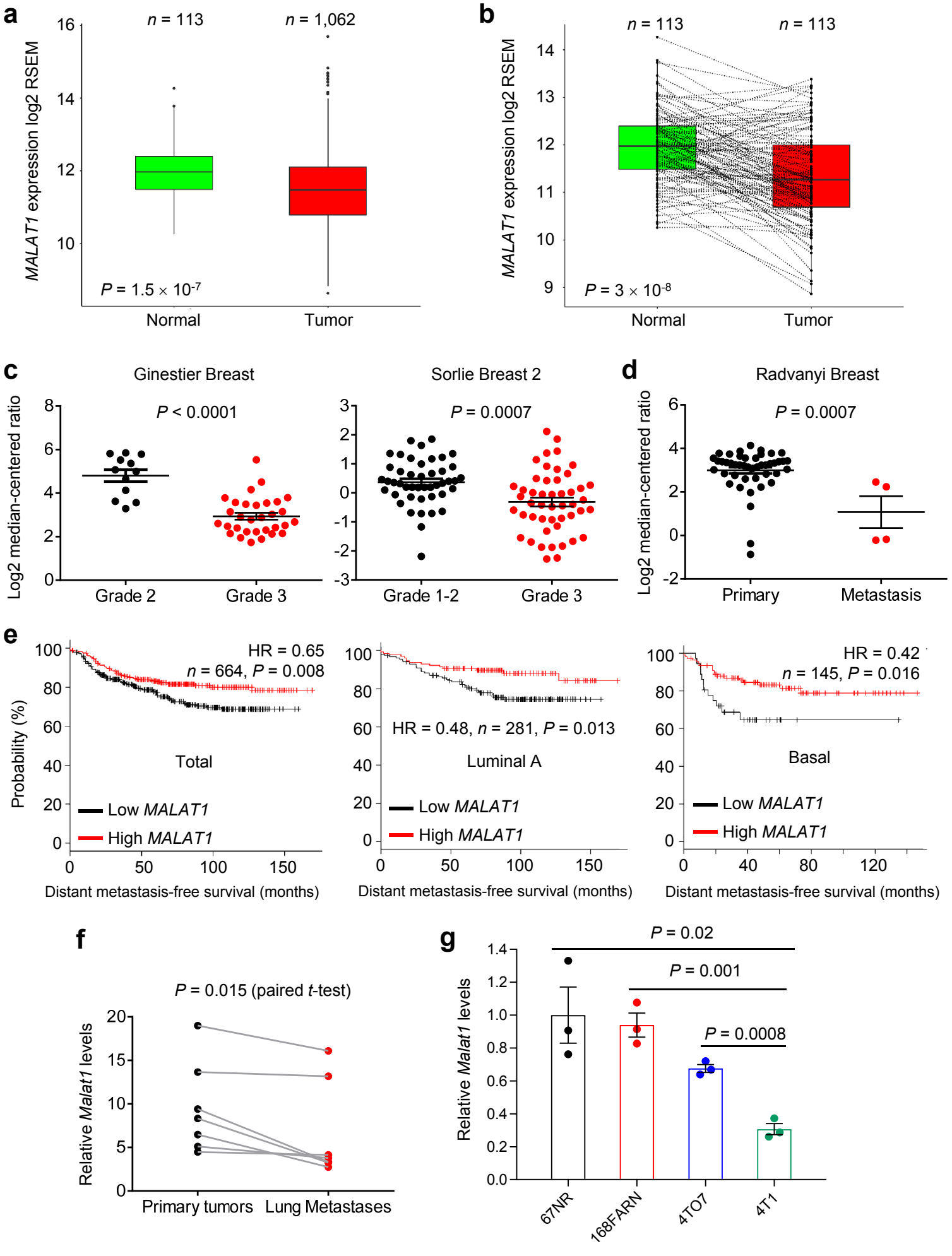
a
n = 113
n = 1,062
MALAT1 expression log2 RSEM
P = 1.5 × 10-7
Normal
Tumor
b
n = 113
n = 113
MALAT1 expression log2 RSEM
P = 3 × 10-8
Normal
Tumor
c
Ginestier Breast
P < 0.0001
Log2 median-centered ratio
Grade 2
Grade 3
Sorlie Breast 2
P = 0.0007
Grade 1-2
Grade 3
d
Radvanyi Breast
P = 0.0007
Log2 median-centered ratio
Primary
Metastasis
e
HR = 0.65
n = 664, P = 0.008
Total
Low MALAT1
High MALAT1
Probability (%)
Distant metastasis-free survival (months)
HR = 0.48, n = 281, P = 0.013
Luminal A
Low MALAT1
High MALAT1
Distant metastasis-free survival (months)
HR = 0.42
n = 145, P = 0.016
Basal
Low MALAT1
High MALAT1
Distant metastasis-free survival (months)
f
P = 0.015 (paired t-test)
Relative Malat1 levels
Primary tumors
Lung Metastases
g
P = 0.02
P = 0.001
P = 0.0008
Relative Malat1 levels
67NR
168FARN
4TO7
4T1

Supplementary Figure 6

***MALAT1* levels are negatively associated with breast cancer progression and metastasis.**

(**a, b**) Unpaired (**a**, *n* = 113 patients for normal tissues; *n* = 1,062 patients for tumor tissues) and paired (**b**, *n* = 113 patients per group) comparison of *MALAT1* levels in normal mammary tissues and breast tumors, based on the RNA-Seq data from TCGA. Statistical significance was determined by an unpaired (**a**) or paired (**b**) Wilcoxon test. The boxes show the median and interquartile range. The whiskers show the minimum and maximum. (**c**) *MALAT1* levels were significantly lower in high-grade breast tumors than in low-grade tumors, based on the Ginestier Breast (*n* = 12 patients for Grade 2; *n* = 31 patients for Grade 3) and Sorlie Breast 2 (*n* = 45 patients for Grade 1-2; *n* = 48 patients for Grade 3) datasets from Oncomine. (**d**) *MALAT1* levels were significantly lower in metastases (*n* = 4 patients) than in primary breast tumors (*n* = 45 patients), based on the Radvanyi Breast dataset from Oncomine. (**e**) Kaplan-Meier curves of distant metastasis-free survival of breast cancer patients (left panel, *n* = 664 patients) and patients of luminal A (middle panel, *n* = 281 patients) or basal (right panel, *n* = 145 patients) subtypes, stratified by *MALAT1* (probe: 223940_x_at) expression levels. Data were obtained from the KM Plotter (see URLs). Auto-select best cutoff was used in the analysis. Statistical significance was determined by a log-rank test. HR is the hazard ratio. (**f**) *Malat1* levels in tumor cells metastasized to lungs were lower than those in primary tumors formed by 4T1 cells. *n* = 7 mice per group. (**g**) qPCR of *Malat1* in 67NR (non-metastatic), 168FARN (weakly metastatic), 4TO7 (weakly metastatic), and 4T1 (highly metastatic) mammary tumor cell lines. *n* = 3 technical replicates per group. Results are representative of two independent experiments. Statistical significance in (**c**), (**d**), (**f**), and (**g**) was determined by an unpaired (**c**, **d**, and **g**) or paired (**f**) *t*-test. Error bars are s.e.m.

a

Symbol	iBAQ (*Malat1* pulldown)
Actr1b	0.28
Arg1	1.20
Fam208b	0.08
Gm15455	0.33
Gm5409	0.23
Hmg20a	0.37
Insrr	0.42
Kif21b	0.02
Mettl3	0.25
Nefh	1.30
Obscn	0.01
Plbd1	0.10
Ppp2r2d	0.22
Rabep1	0.02
Tead1	0.18
Tead2	0.21
Tead3	0.15
Tead4	0.18
Try10	0.23
Uchl5	0.12
Ywhab	0.87
Zfp318	0.22
Zfp346	0.79

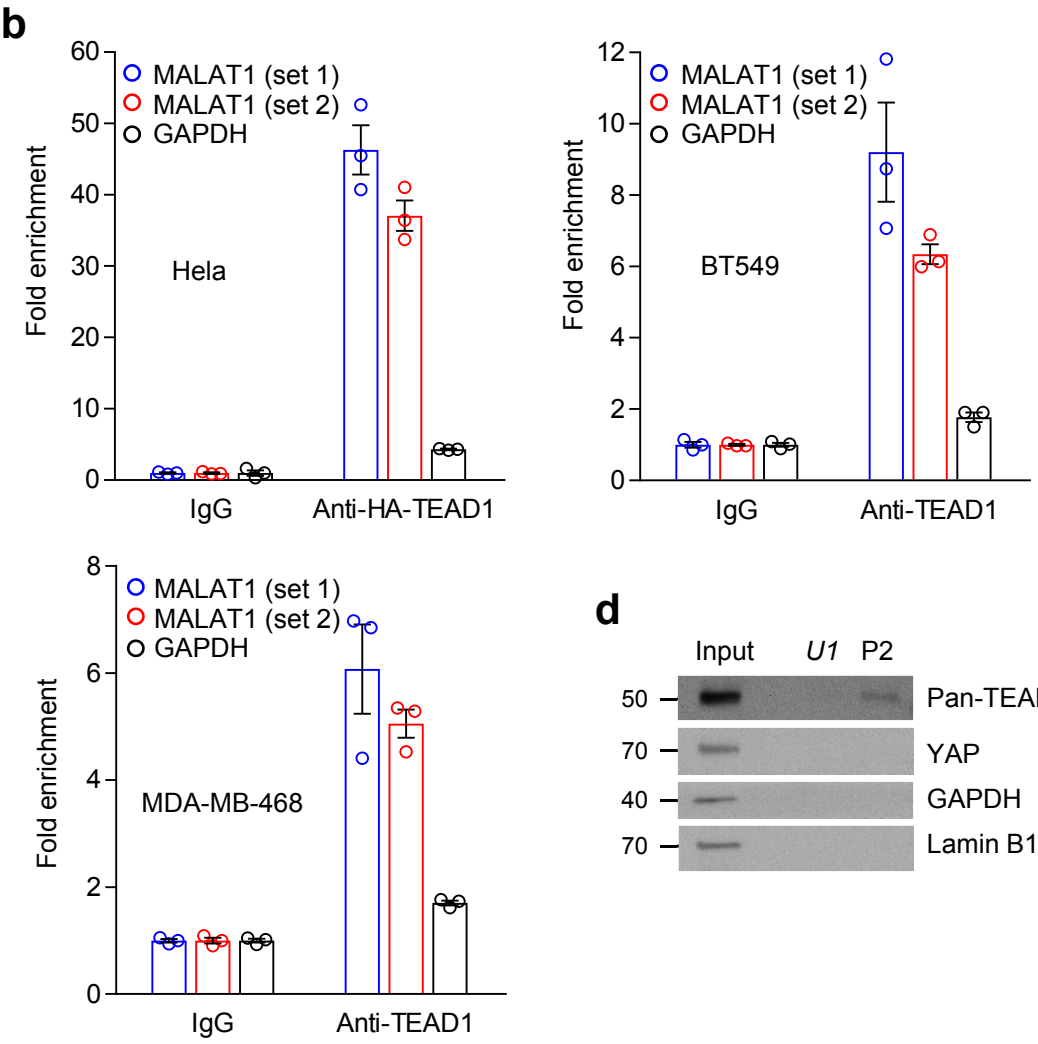

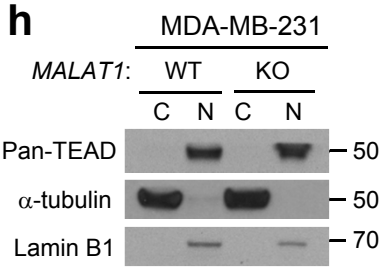

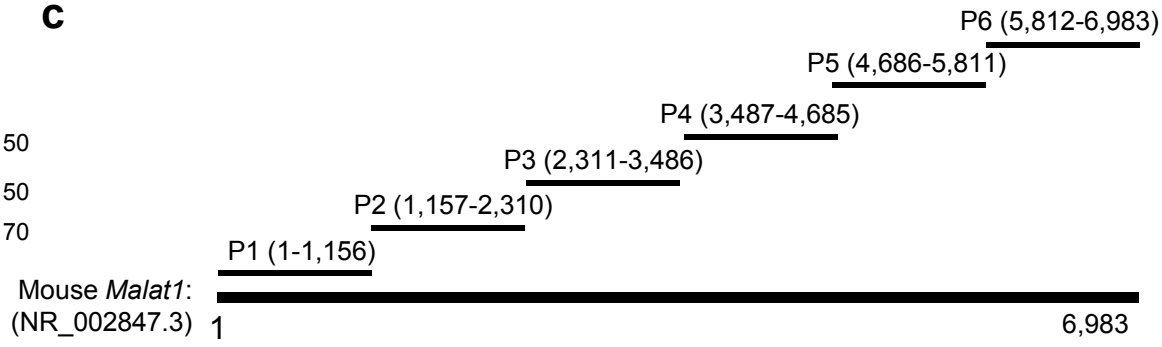

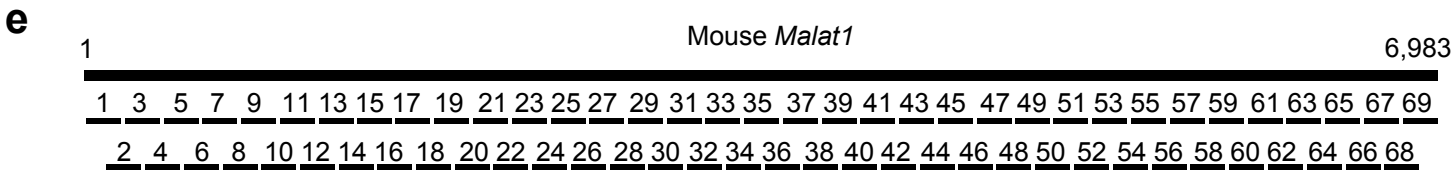

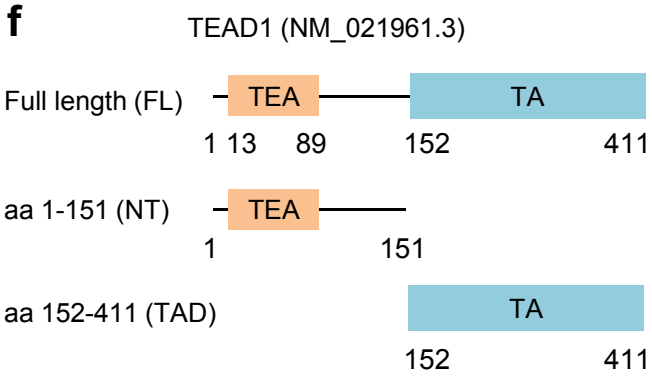

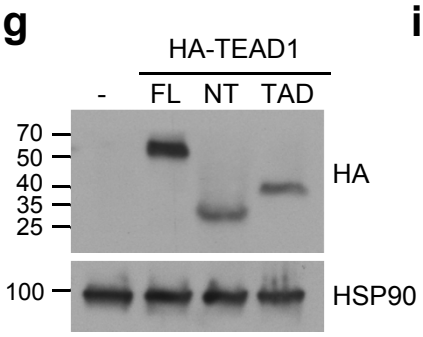

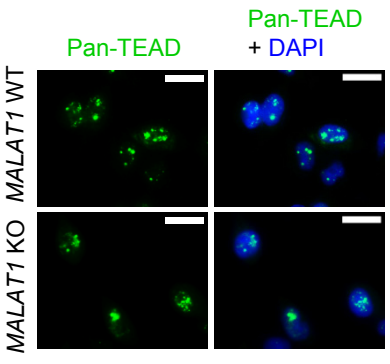

Supplementary Figure 7

***MALAT1* interacts with TEAD proteins.**

(**a**) A list of proteins bound to *Malat1* but not *U1* or streptavidin beads (no probes) from ChIRP-MS analysis of PyMT mammary tumor samples. (**b**) RNA immunoprecipitation assays. Cells (Hela transfected with HA-TEAD1, BT549, and MDA-MB-468) were crosslinked and subjected to immunoprecipitation with an antibody against TEAD1 (for BT549 and MDA-MB-468) or HA (for Hela). TEAD1-bound *MALAT1* was quantitated by qPCR with two primer sets. *GAPDH* was used as a negative control. Error bars are s.e.m. of three technical replicates per group and results are representative of two independent experiments. (**c**) Location of the six mouse *Malat1* fragments used in **Fig. 4e**. (**d**) RNA pulldown assay. Biotinylated *Malat1* fragment (P2) and nuclear RNA *U1* were synthesized by *in vitro* transcription, incubated with HEK293FT cell lysate, and pulled down with streptavidin beads. The bound proteins were eluted by boiling in Laemmli sample buffer and immunoblotted with antibodies against pan-TEAD, YAP, GAPDH, and Lamin B1. Results are representative of two independent experiments. (**e**) Schematic representation of mouse *Malat1* segments amplified by 69 primer pairs for CLIP-qPCR shown in **Fig. 4f**. (**f**) Schematic representation of full-length (FL) human TEAD1 and two truncation mutants, NT (N-terminal region) and TAD (C-terminal transactivation domain). (**g**) HA-tagged full-length TEAD1, N-terminal region, and transactivation domain were transfected into Hela cells and their expression was examined by immunoblotting with an HA-specific antibody. Results are representative of three independent experiments. (**h**) Immunoblotting of pan-TEAD, α-tubulin (cytoplasmic marker), and Lamin B1 (nuclear marker) in cytoplasmic and nuclear fractions of control and *MALAT1* knockout MDA-MB-231 cells. Results are representative of two independent experiments. (**i**) Immunofluorescent staining of pan-TEAD (green) in control and *MALAT1* knockout MDA-MB-231 cells. The right column is the overlay of TEAD and nuclear DAPI (blue) staining of the same field. Images are representative of four random fields per group and results are representative of two independent experiments. Scale bars, 20 μm. Uncropped blots are shown in **Supplementary Fig. 10**.

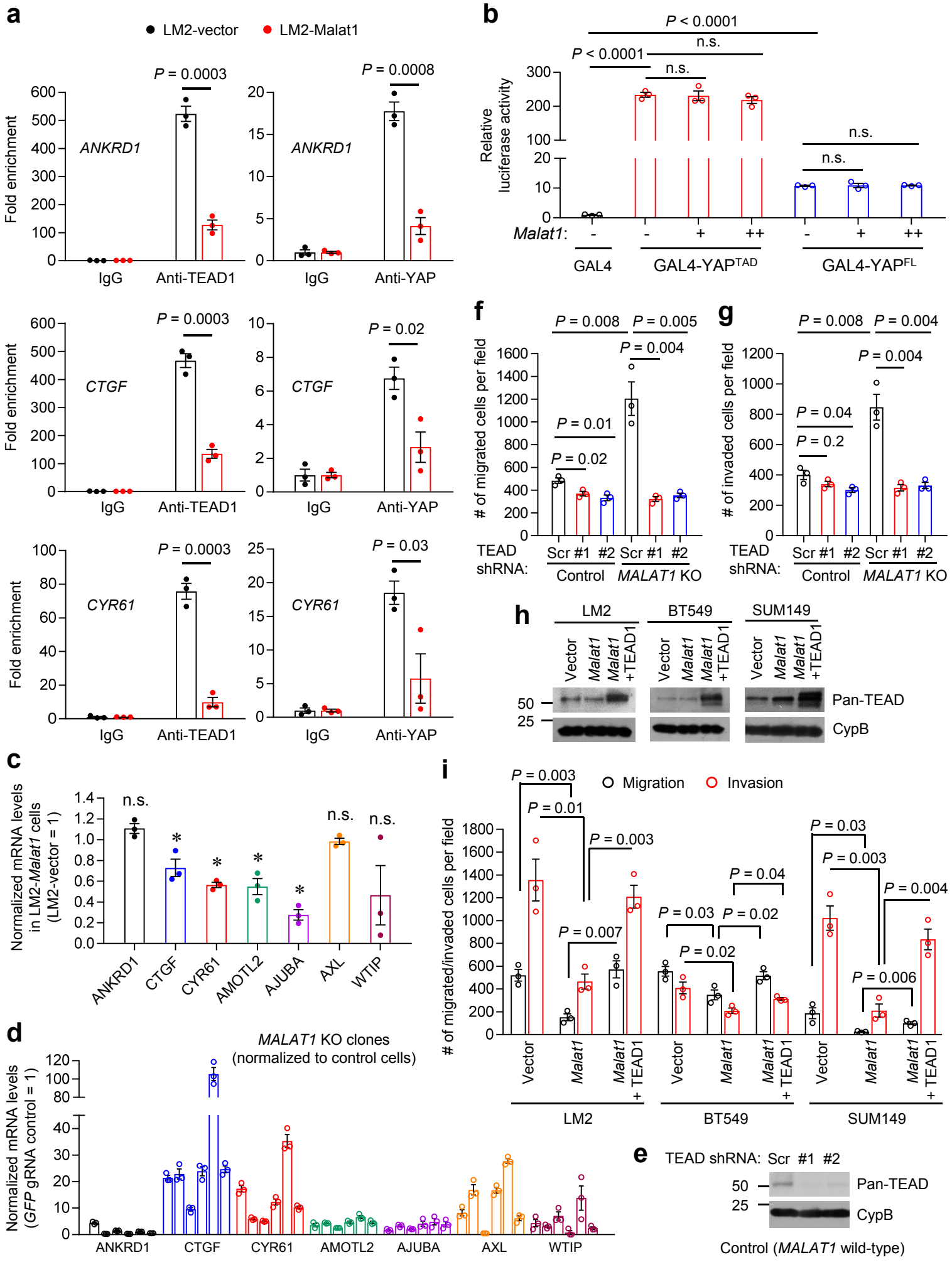
a
LM2-vector
LM2-Malat1
ANKRD1
CTGF
CYR61
Fold enrichment
P = 0.0003
P = 0.0008
P = 0.02
P = 0.03
IgG
Anti-TEAD1
Anti-YAP
b
Relative luciferase activity
P < 0.0001
n.s.
Malat1:
GAL4
GAL4-YAP^TAD
GAL4-YAP^FL
c
Normalized mRNA levels in LM2-Malat1 cells (LM2-vector = 1)
ANKRD1
CTGF
CYR61
AMOTL2
AJUBA
AXL
WTIP
d
MALAT1 KO clones (normalized to control cells)
Normalized mRNA levels (GFP gRNA control = 1)
e
TEAD shRNA: Scr #1 #2
Pan-TEAD
CypB
Control (MALAT1 wild-type)
f
# of migrated cells per field
P = 0.008
P = 0.005
P = 0.004
P = 0.01
P = 0.02
TEAD shRNA:
Control
MALAT1 KO
g
# of invaded cells per field
P = 0.04
P = 0.2
h
LM2
BT549
SUM149
Vector
Malat1
Malat1 +TEAD1
50
25
i
Migration
Invasion
# of migrated/invaded cells per field
P = 0.003
P = 0.007
P = 0.03
P = 0.02
P = 0.006

Supplementary Figure 8

***MALAT1* inhibits TEAD.**

(**a**) ChIP-qPCR analysis showing the occupancy of *ANKRD1*, *CTGF*, and *CYR61* promoters by TEAD1 or YAP. Endogenous TEAD1 and YAP were immunoprecipitated from control or *Malat1*-expressing LM2 cells. n = 3 technical replicates per group. Results are representative of two independent experiments. (**b**) Luciferase activity in HEK293FT cells co-transfected with mouse *Malat1*, GAL4 DBD alone or GAL4 DBD-fused protein (full-length YAP or its transactivation domain), a pG5-luciferase reporter containing 5× GAL4-binding sites, and a Renilla luciferase reporter (for normalization). n = 3 cell culture replicates per group. Results are representative of two independent experiments. (**c**) qPCR of seven classical YAP-TEAD target genes in *Malat1*-overexpressing LM2 cells. Data are normalized to the control cells. n = 3 technical replicates per group. Results are representative of two independent experiments. (**d**) qPCR of seven classical YAP-TEAD target genes in six *MALAT1* knockout clones of MDA-MB-231 cells. Data are normalized to the control cells expressing *GFP* gRNA. n = 3 technical replicates per group. Results are representative of two independent experiments. (**e**) Immunoblotting of pan-TEAD and cyclophilin B (CypB) in control MDA-MB-231 cells with or without viral infection of shRNA targeting TEAD family members. Scr: scramble control. Results are representative of three independent experiments. (**f, g**) Migration (**f**) and invasion (**g**) assays of control and *MALAT1* knockout MDA-MB-231 cells with or without viral infection of shRNA targeting TEAD family members. Scr: scramble control. n = 3 cell culture replicates per group. Results are representative of two independent experiments. (**h**) Immunoblotting of pan-TEAD and cyclophilin B (CypB) in LM2, BT549, and SUM149 cells transfected with mouse *Malat1* in the presence or absence of HA-tagged human TEAD1. Results are representative of two independent experiments. (**i**) Migration and invasion assays of LM2, BT549, and SUM149 cells transfected with mouse *Malat1* in the presence or absence of HA-tagged human TEAD1. n = 3 cell culture replicates per group. Results are representative of two independent experiments. Statistical significance in (**a**)-(**c**), (**f**), (**g**), and (**i**) was determined by an unpaired t-test. Error bars are s.e.m. *: $P < 0.05$; n.s.: not significant ($P \geq 0.05$). Uncropped blots are shown in **Supplementary Fig. 10**.

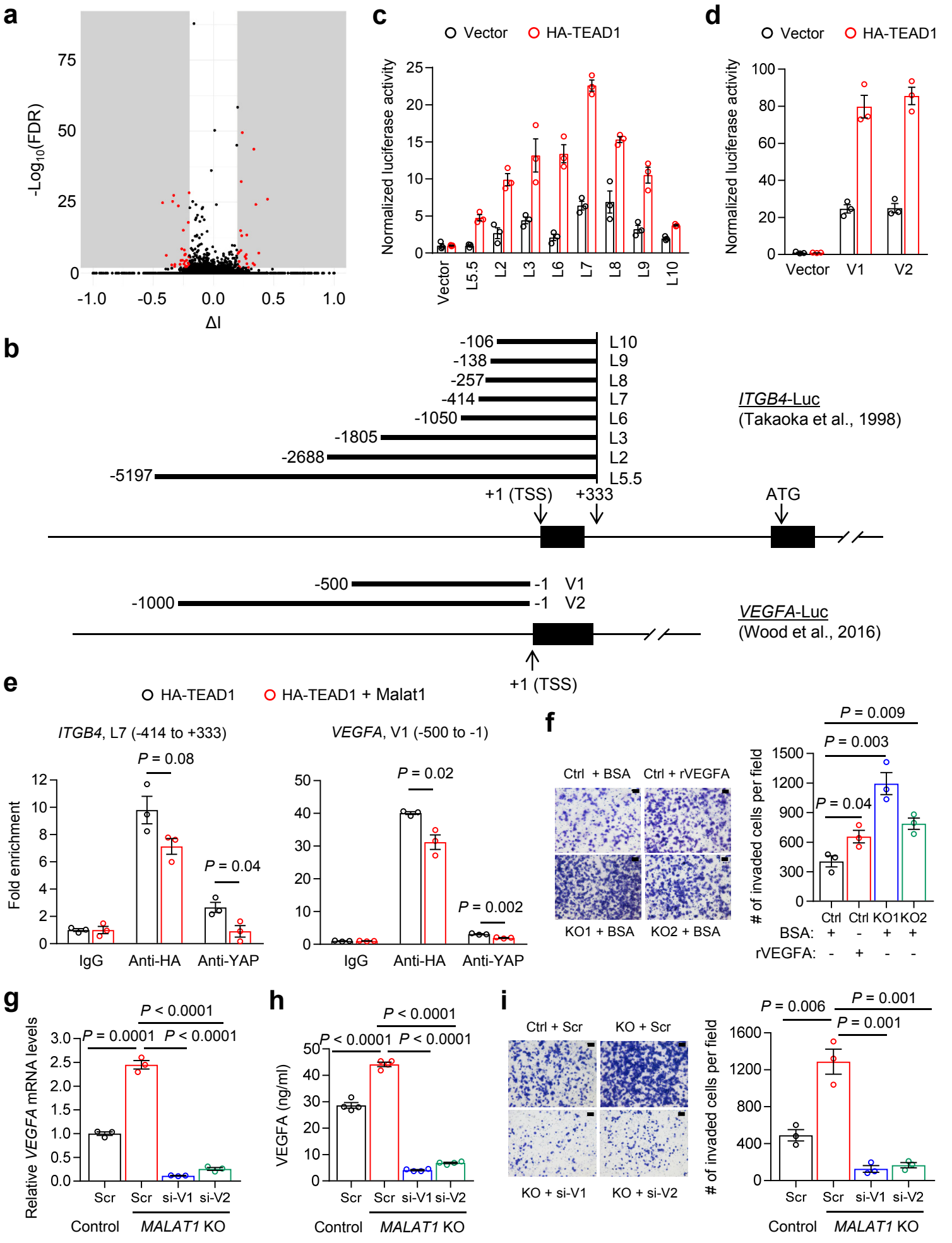
a
-Log10(FDR)
ΔI
c
Vector
HA-TEAD1
Normalized luciferase activity
Vector
L5.5
L2
L3
L6
L7
L8
L9
L10
d
Vector
HA-TEAD1
Normalized luciferase activity
Vector
V1
V2
b
-106
-138
-257
-414
-1050
-1805
-2688
-5197
L10
L9
L8
L7
L6
L3
L2
L5.5
+1 (TSS)
+333
ATG
ITGB4-Luc
(Takaoka et al., 1998)
-500
-1000
-1
-1
V1
V2
VEGFA-Luc
(Wood et al., 2016)
+1 (TSS)
e
HA-TEAD1
HA-TEAD1 + Malat1
ITGB4, L7 (-414 to +333)
P = 0.08
P = 0.04
Fold enrichment
IgG
Anti-HA
Anti-YAP
VEGFA, V1 (-500 to -1)
P = 0.02
P = 0.002
IgG
Anti-HA
Anti-YAP
f
Ctrl + BSA
Ctrl + rVEGFA
KO1 + BSA
KO2 + BSA
P = 0.009
P = 0.003
P = 0.04
# of invaded cells per field
Ctrl
Ctrl
KO1
KO2
BSA:
rVEGFA:
g
P < 0.0001
P = 0.0001
P < 0.0001
Relative VEGFA mRNA levels
Scr
Scr
si-V1
si-V2
Control
MALAT1 KO
h
P < 0.0001
P < 0.0001
P < 0.0001
VEGFA (ng/ml)
Scr
Scr
si-V1
si-V2
Control
MALAT1 KO
i
Ctrl + Scr
KO + Scr
KO + si-V1
KO + si-V2
P = 0.006
P = 0.001
P = 0.001
# of invaded cells per field
Scr
Scr
si-V1
si-V2
Control
MALAT1 KO

Supplementary Figure 9

***ITGB4* and *VEGFA* are TEAD target genes that are regulated by *MALAT1*.**

(**a**) Volcano plot showing the proportional change of inclusion level of the exons (x-axis) and their statistical significance (y-axis) upon *Malat1* loss. In total, 51 of 16,034 cassette exons exhibited significant changes in the splicing pattern in *Malat1* knockout PyMT tumors compared with *Malat1* wild-type PyMT tumors. Fisher's exact test was performed. Statistically significant changes were defined using the cutoff values recommended by the software used: false discovery rate, FDR < 0.01, and proportional change of inclusion level, $|\Delta I| > 0.2$. Red dots and shaded areas indicate statistically significant changes. (**b**) Putative promoter regions of the human *ITGB4* (upper panel) and *VEGFA* (lower panel) genes cloned into a luciferase reporter plasmid. Black boxes indicate exons. (**c, d**) Luciferase activity in HEK293FT cells co-transfected with HA-TEAD1, the *ITGB4* (**c**) or *VEGFA* (**d**) luciferase reporter, and a Renilla luciferase reporter (for normalization). *n* = 3 cell culture replicates per group. Results are representative of two independent experiments. (**e**) ChIP-qPCR analysis showing the occupancy of *ITGB4* (L7, left panel) and *VEGFA* (V1, right panel) promoters by TEAD1 or YAP. Ectopically expressed HA-TEAD1 and endogenous YAP were immunoprecipitated from Hela cells with or without ectopic expression of *Malat1*. *n* = 3 technical replicates per group. Results are representative of two independent experiments. (**f**) Images (left panel) and data quantification (right panel) of migration and invasion assays of control and *MALAT1* knockout MDA-MB-231 cells treated with bovine serum albumin (BSA) or recombinant human $VEGFA_{165}$. *n* = 3 cell culture replicates per group. Results are representative of two independent experiments and images are representative of three random fields per group. Scale bars, 100 μm. (**g**) qPCR of *VEGFA* in control and *MALAT1* knockout MDA-MB-231 cells transfected with a scramble control (Scr) or siRNAs against VEGFA (si-V1 and si-V2). *n* = 3 technical replicates per group. Results are representative of two independent experiments. (**h**) ELISA of VEGFA secreted by control and *MALAT1* knockout MDA-MB-231 cells transfected with a scramble control (Scr) or siRNAs against VEGFA (si-V1 and si-V2). *n* = 4 cell culture replicates per group. Results are representative of two independent experiments. (**i**) Images (left panel) and data quantification (right panel) of migration and invasion assays of control and *MALAT1* knockout MDA-MB-231 cells transfected with a scramble control (Scr) or siRNAs against VEGFA (si-V1 and si-V2). *n* = 3 cell culture replicates per group. Results are representative of two independent experiments and images are representative of three random fields per group. Scale bars, 100 μm. Statistical significance in (**e**)-(**i**) was determined by an unpaired *t*-test. Error bars are s.e.m.

Figure 4b

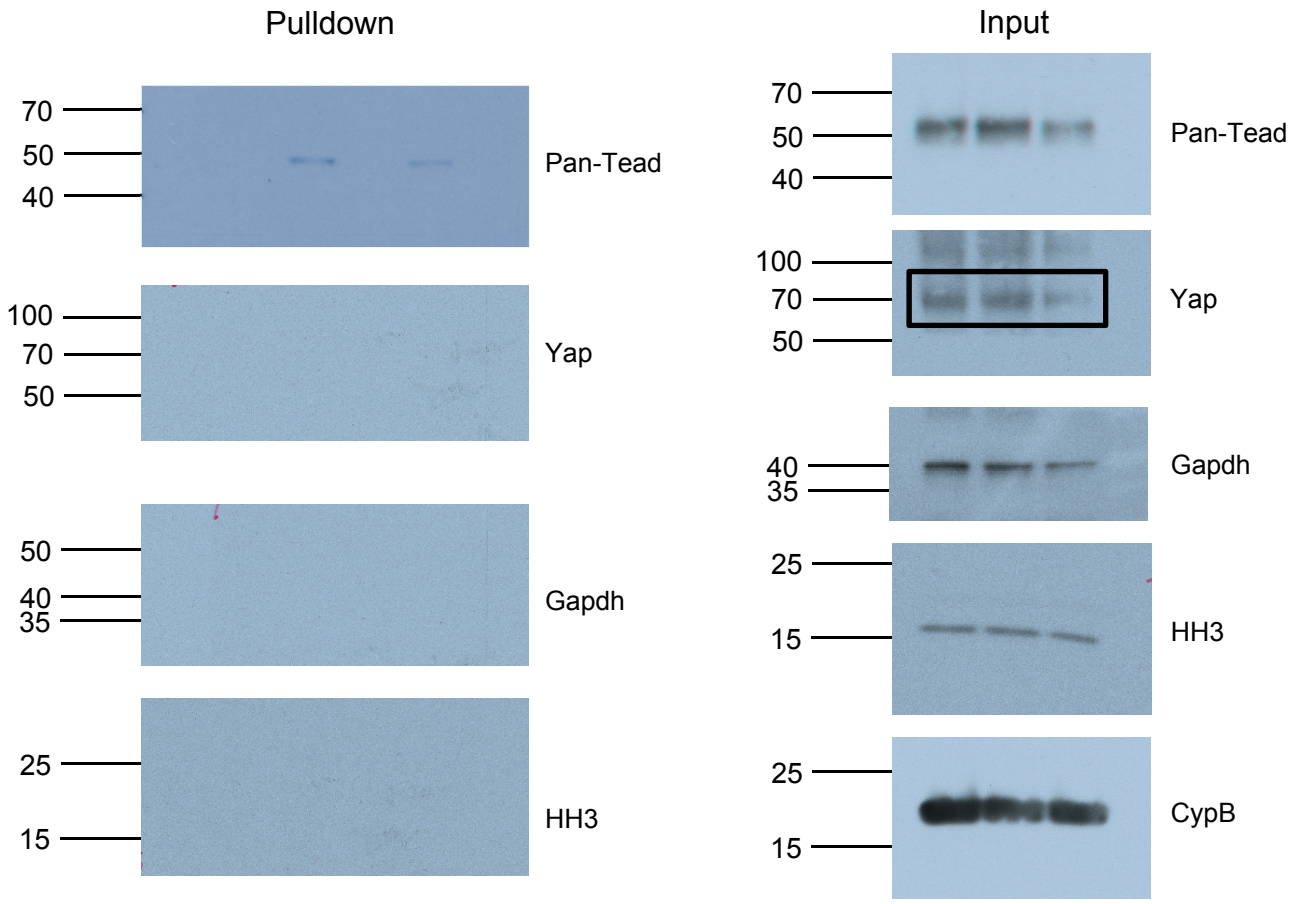

Figure 4c

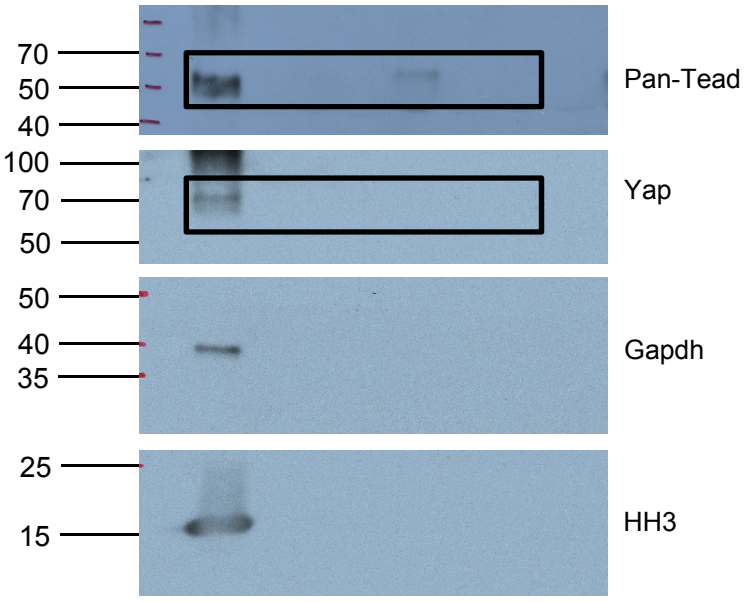

Figure 4e

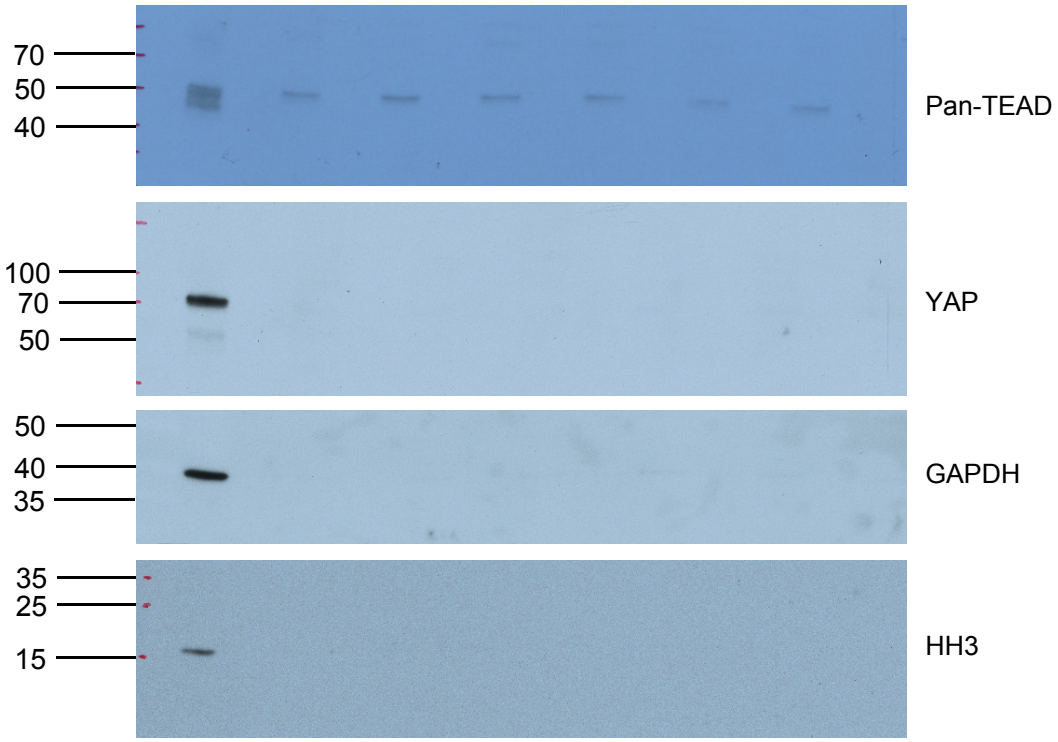

Figure 5c

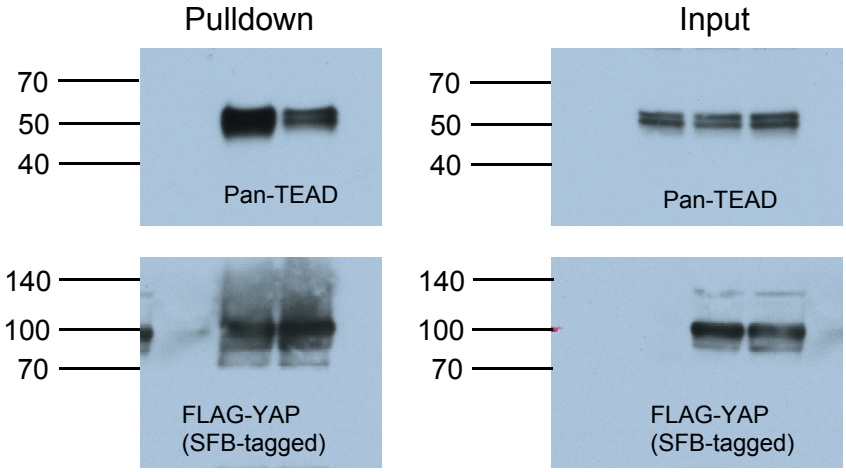

Figure 5d

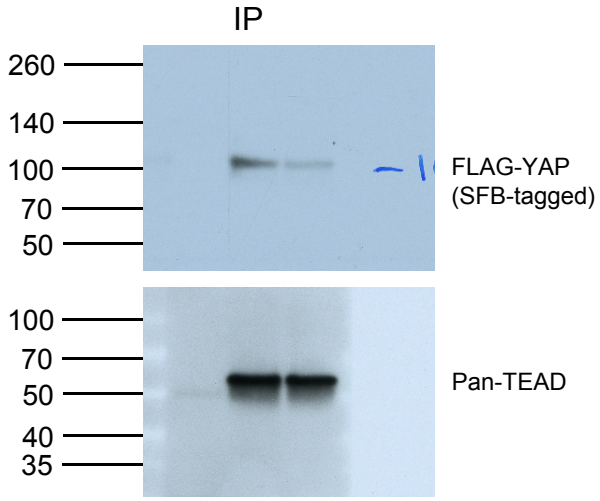

Figure 5g

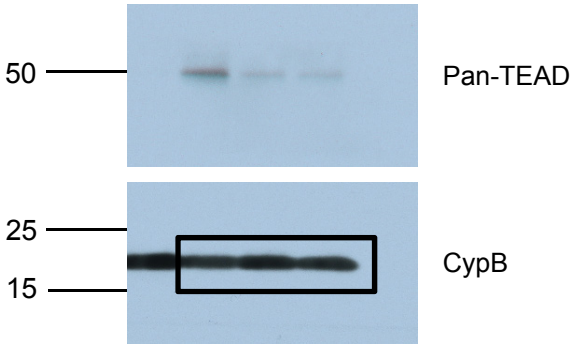

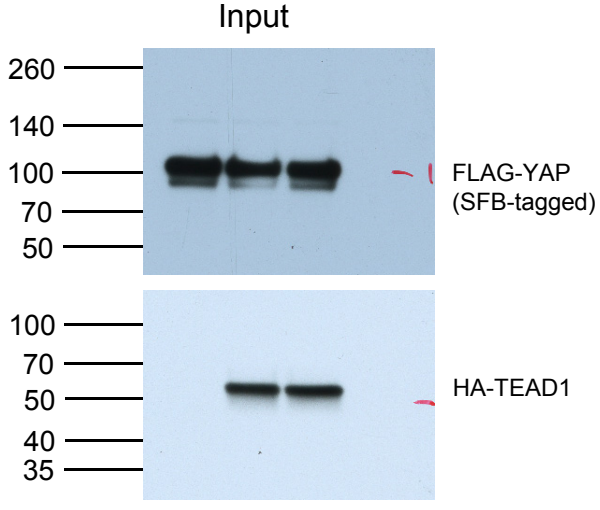

Supplementary Figure 7d

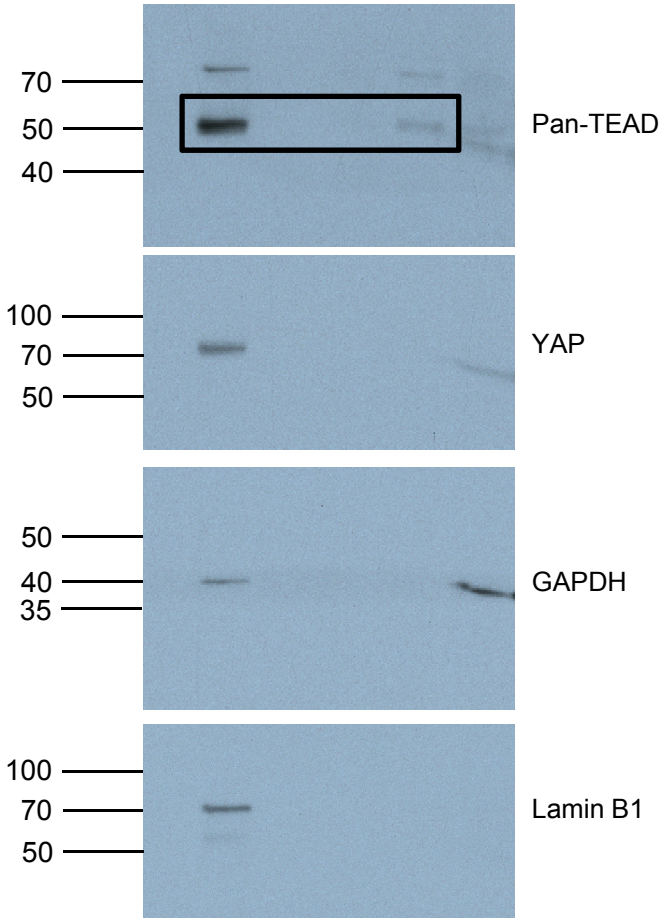

Supplementary Figure 7g

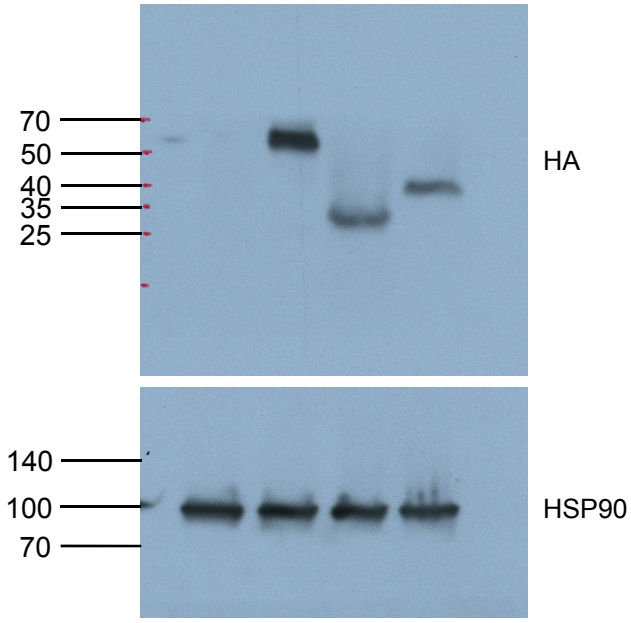

Supplementary Figure 7h

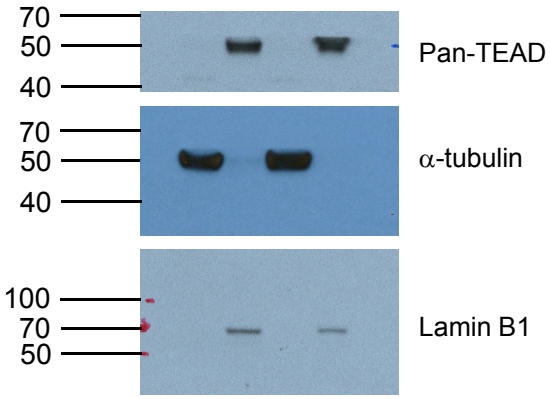

Supplementary Figure 8e

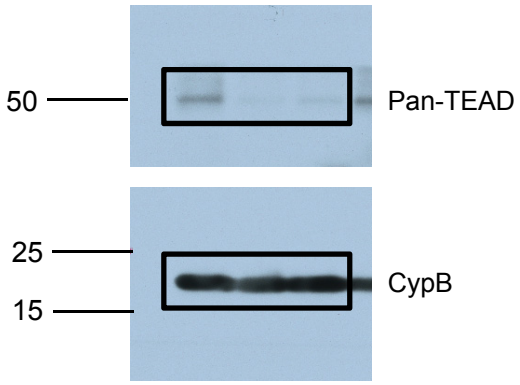

Supplementary Figure 8h

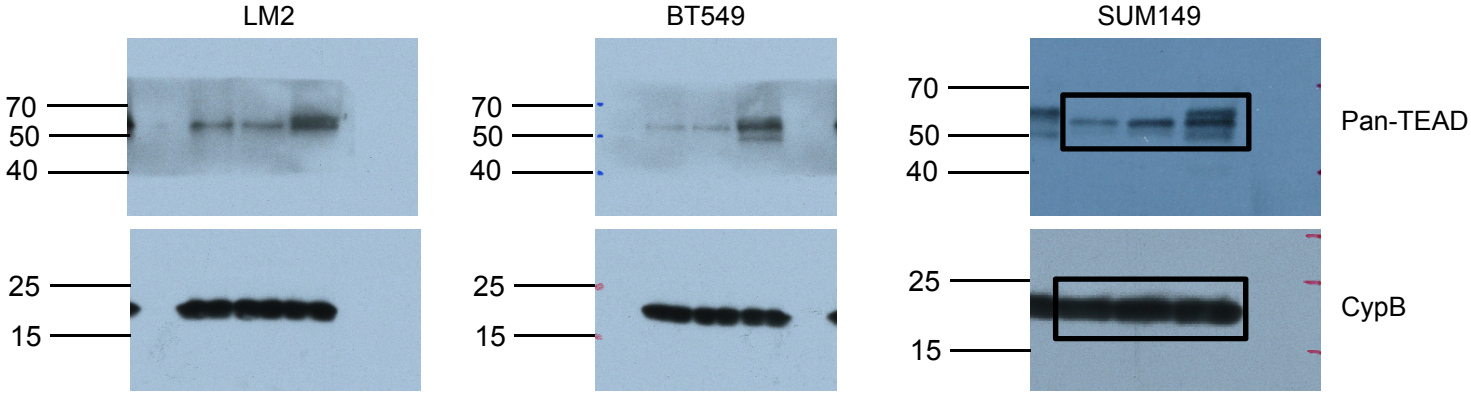

Supplementary Figure 10. Uncropped blots.

Supplementary Table 1. mRNA fold change (LM2-control/LM2-Malat1) based on the qPCR array

Gene	Control/Malat1
APC	0.526270344
BRMS1	0.604526446
CCL7	4.360787837
CD44	0.518205459
CDH1	1.337401685
CDH11	2.585520917
CDH6	0.217133111
CDKN2A	2.585520917
CHD4	2.585520917
COL4A2	0.396219694
CST7	0.399438199
CTBP1	0.700696912
CTNNA1	0.494847211
CTSK	0.580296722
CTSL	0.507223084
CXCL12	0.51173037
CXCR4	0.122569265
DENR	0.055947859
EPHB2	0.180205258
ETV4	0.656723362
EWSR1	0.609090851
FAT1	0.017544339
FGFR4	0.358643933
FLT4	0.249496246
FN1	0.042127897
FXYD5	2.585520917
GNRH1	0.401304009
KISS1R	0.727271514
HGF	0.855125512
HPSE	2.585520917
HRAS	0.576373407
HTATIP2	0.479871458
IGF1	0.540112852
IL18	0.042025455
IL1B	0.334871509
CXCR2	2.150318077
ITGA7	0.037639319
ITGB3	0.907664478
CD82	0.671827866
KISS1	0.465682533
KRAS	0.6744075
RPSA	1.503094985
MCAM	0.45554935
MDM2	0.553380803

Gene	Control/Malat1
MET	0.612124568
METAP2	0.516735826
MGAT5	0.4893427
MMP10	0.015778633
MMP11	6.97991132
MMP13	0.678637241
MMP2	1.373487215
MMP3	0.991957631
MMP7	3.18656406
MMP9	0.648749093
MTA1	0.213073219
MTSS1	0.542352478
MYC	0.684157825
MYCL	0.617973183
NF2	0.814863484
NME1	0.540708416
NME2	0.462755962
NME4	1.271427942
NR4A3	1.013682469
PLAUR	0.810873159
PNN	1.123465017
PTEN	0.493344987
RB1	0.685453727
RORB	0.954084461
SET	0.789142533
SMAD2	0.864600232
SMAD4	0.591694781
SRC	0.783310995
SSTR2	0.407998258
SYK	2.585520917
TCF20	1.247630486
TGFB1	0.86181454
TIMP2	0.978463612
TIMP3	1.473566961
TIMP4	0.643171691
TNFSF10	0.701470341
TP53	0.810986678
TRPM1	2.585520917
TSHR	19.12182959
VEGFA	4.195898665

: Ct > 35

: Ct < 35 and fold change > 2

Supplementary Table 2. Primer, gRNA, and shRNA sequences

Use	Gene	Direction	Sequence (5' → 3')
Human RNA qPCR	*MALAT1* set 0	Forward	GGTTCAGAAGGTCTGAAGCTC
		Reverse	CCCAGAAGTGTTTACACTGCT
	MALAT1 set 1	Forward	GCATTAATTGACAGCTGACCCA
		Reverse	GCTTGCTCCTCAGTCCTAGCTT
	MALAT1 set 2	Forward	GAGCGAGTGCAATTTGGTGATG
		Reverse	ATCCTCTACGCACAACGCC
	MALAT1 set 3	Forward	GCCAAATTGAGACAATTTCAGC
		Reverse	CGAATTCAGGGTGAGGAAGTA
	MALAT1 set 4	Forward	CTGAGTCATAACCAGCCTGGC
		Reverse	GCTTATTCCCCAATGGAGGTA
	CTGF	Forward	CGACTGGAAGACACGTTTGG
		Reverse	AGGCTTGGAGATTTTGGGAG
	CYR61	Forward	GAGTGGGTCTGTGACGAGGAT
		Reverse	GGTTGTATAGGATGCGAGGCT
	ANKRD1	Forward	CACTTCTAGCCCACCCTGTGA
		Reverse	CCACAGGTTCCGTAATGATTT
	AXL	Forward	TTTATGACTATCTGCGCCAGG
		Reverse	TGTGTTCTCCAAATCTTCCCG
	AMOTL2	Forward	GACTTCAACCGGGATCTTAGAG
		Reverse	CCAGCTTCTCTTGCTCCTG
	AJUBA	Forward	TGTCAATGGCTCTGTGTACTG
		Reverse	ATGATAGGACTTCCCCATTGC
	WTIP	Forward	GCGAGACTATCACACGGTTT
		Reverse	TCCTCACAGTGGTAACATGC
	ITGB4	Forward	AGCCTTGATCAGCGTCAG
		Reverse	AACATCTCGTCTGTGCAGTAG
	VEGFA	Forward	AGTCCAACATCACCATGCAG
		Reverse	TTCCCTTTCCTCGAACTGATTT
	LTBP3	Forward	TCCCACTCAGGTCACAGAG
		Reverse	TTCACATCCACGCAGTAGC
	TIGD3	Forward	GCACTTCTCCTGAGCTATTCG
		Reverse	CCGATCTGCCTTCTGAAGAG
	FRMD8	Forward	ATCTTGTGGCTGGAGTTCG
		Reverse	GCTCAGTTCGATGCAGTACTC
	EHBP1L1	Forward	CGAGCTAGTGTTGGAGTGC
		Reverse	CGGTATGGGTTCTGGATGC

	NEAT1	Forward	GTGGCTGTTGGAGTCGGTAT
		Reverse	TAACAAACCACGGTCCATGA
	MAP3K11	Forward	ATGTGCTGGTCAACTGGG
		Reverse	CGTCACTCTCAATGGGCTG
	KCNK7	Forward	CAACAGCTCAGAGGGCAG
		Reverse	CATAGACCATGCAGAAGGCC
	FAM89B	Forward	CTGTCAACCTCGACTCAGC
		Reverse	GCAGAAGCTCAGGTCTTGG
	SCYL1	Forward	AGCAGTTCATCCAGTACCTTG
		Reverse	TGGCCTCGTTCAGCTTTG
	SLC25A45	Forward	ACAACCCTGAAGAGAACAGC
		Reverse	TGCAGCCTCACCTTTACAG
	DPF2	Forward	GAACAGGGAAGATGGCGG
		Reverse	TGTGAGTCCAAGAAAGGCAG
	CDC42EP2	Forward	ACTCTGTAAGTTCACCGCC
		Reverse	ACTTTGGTCTTGTCACCGAG
	GAPDH (for normalization)	Forward	ACATCGCTCAGACACCATG
		Reverse	TGTAGTTGAGGTCAATGAAGGG
Mouse RNA qPCR	*Malat1*	Forward	ACCTCCCAGTTTTGTAAGACG
		Reverse	CCAATTACCTCCCCTACACAG
	Ctgf	Forward	CTCCACCCGAGTTACCAATG
		Reverse	TGGCGATTTTAGGTGTCCG
	Cyr61	Forward	GGGTTGGAATGCAATTTCGG
		Reverse	TGGTGTTTACAGTTGGGCTG
	Ankrd1	Forward	TGCGATGAGTATAAACGGACG
		Reverse	TGGATGGCTGTGGATTCAAG
	Axl	Forward	GTGGAAAGAGGTGAACTGGTAG
		Reverse	GTCTCGTAGTTTCTCCTTCAGC
	Amotl2	Forward	AGATGGAGACTGTACTGAGGG
		Reverse	GAGCCGCTGGATTTCATTTTC
	Ajuba	Forward	GGTATCTATGGGCAGAGCAATG
		Reverse	CAGTAGACAGAGCCATTGACG
	Wtip	Forward	ATCACACCGACTGCTTCATC
		Reverse	ACACGCTACACTTGTCAGC
	Itgb4	Forward	TCTGCTATGGACTGGTCAATG
		Reverse	GTATCGGTATGGCTGGGATTC
	Vegfa	Forward	GGCAGCTTGAGTTAAACGAAC
		Reverse	TGGTGACATGGTTAATCGGTC
	Tigd3	Forward	GTCACTCTCTGGTTCTGCTG

		Reverse	GCACCTGGATCTTCTCAGC
	Ltbp3	Forward	CAGGGTCATCGGTTGGTG
		Reverse	GTCCTGGGTGAGTGTGAAAC
	Neat1	Forward	TTGGGACAGTGGACGTGTGG
		Reverse	TCAAGTGCCAGCAGACAGCA
	Frmd8	Forward	GAATTTGTCCTCAATCAGTGCC
		Reverse	TTTATAGGGCTGGTGCTTGG
	Ehbp1l1	Forward	GTTTGTGGCGTGTTACCATG
		Reverse	CACGGTATGGGTTCTGGATG
	Scyl1	Forward	GAGCAGTTCATCCAATACCTTG
		Reverse	TGGCCTCATTCAGCTTTGG
	Kcnk7	Forward	AGACAAGCAACTGGGATCTG
		Reverse	CTGCATAGACCACACAGAAGG
	Fam89b	Forward	GGCCTTCTTAACGCTAGTGGG
		Reverse	AGAACCTGAGTTAGCAGATCCAG
	Slc25a45	Forward	ATCTCACTTGCAACAGTCTCC
		Reverse	ACCTTTACAGTGTCGAATGGG
	Map3k11	Forward	ACCTGATGCCCATAGTTCAC
		Reverse	CAGAGCGTGATATTCCTGGTG
	Dpf2	Forward	CTGGGCGAGTTTCCTGTTAG
		Reverse	CTGCTCACACCCTTACTCTTG
	Cdc42ep2	Forward	TCCCCATCTATTTGAAACGTGG
		Reverse	CCGCTGTTCCTGGAAGGAG
	Ribosomal RNA 15 (for normalization)	Forward	CTTCCGCAAGTTCACCTACC
		Reverse	TACTTGAGGGGGATGAATCG
ChIP-qPCR	*ANKRD1*	Forward	GAGGGGAGGACAAGCTAACC
		Reverse	CGATGTGATCACCACCAAAG
	CTGF	Forward	GCCAATGAGCTGAATGGAGT
		Reverse	CAATCCGGTGTGAGTTGATG
	CYR61	Forward	AGCAAACAGCTCACTGCCTT
		Reverse	ATGGTAGTTGGAGGGTCGTG
	ITGB4 (-414 to +333)	Forward	GGCACCCAGCTCCTG
		Reverse	AGCGCTTTATGGGGCG
	VEGFA (-500 to -1*)*	Forward	CGGGTTTTATCCCTCTTCTTTTTTC
		Reverse	CAATCTCCCCAAGCCGTC
gRNA	*MALAT1* gRNA#1		GCTGGGGCTCAGTTGCGTAA
	MALAT1 gRNA#2		AGGTTTCTAAAACATGACGG
	GFP gRNA#1		GAGCTGGACGGCGACGTAAA
	GFP gRNA#2		CAGAACACCCCCATCGGCGA
Cloning sh-TEAD	sh-TEAD1/3/4 #1	Sense	CCGGATGATCAACTTCATCCACAA GCTCGAGCTTGTGGATGAAGTTGA

			TCATTTTTTC
		Antisense	AATTGAAAAAATGATCAACTTCATC CACAAGCTCGAGCTTGTGGATGAA GTTGATCAT
	sh-TEAD1/3/4 #2	Sense	CCGGGATCAACTTCATCCACAAGC TCTCGAGAGCTTGTGGATGAAGTT GATCTTTTTC
		Antisense	AATTGAAAAAGATCAACTTCATCCA CAAGCTCTCGAGAGCTTGTGGATG AAGTTGATC
Cloning mutant TEAD1 (NT)	TEAD1 (NT)	Forward	TTCAAACAGGGCAGCCATGAGAATTCCGCCC C
		Reverse	GGGGCGGAATTCTCATGGCTGCCCTGTTTGAA
Cloning mutant TEAD1 (TAD)	TEAD1 (TAD)	Forward	CTCAGTGCGGCCGCGGATCCTCACAAGA
		Reverse	TCTTGTGAGGATCCGCGGCCGCACTGAG
Genotyping	CMV-Cre transgene	Forward	GCGGTCTGGCAGTAAAAACTATC
		Reverse	GTGAAACAGCATTGCTGTCACTT
	Malat1 targeted mutant allele (*Malat1*^{LSL})	Forward	TGGCAGGCTTGAGATCTGG
		Reverse	CCCAAGGCACACAAAAAACC
	Malat1 transgenic allele (*Malat1*^{Tg})	Forward	TGGCAGGCTTGAGATCTGG
		Reverse	CTCTCGCTGCCTGAATGC
	PyMT transgene	Forward	GGAAGCAAGTACTTCACAAGGG
		Reverse	GGAAAGTCACTAGGAGCAGGG
	Malat1 wild-type allele (endogenous)	Forward	CCCACACGACGTCAAGAAAAATC
		Reverse	GCTCTGGTCAGCCTCCATTA
	Malat1 knockout allele (insertional disruption)	Forward	TTGAAGTGGCGAGCGATAC
		Reverse	AGATCCCAGCGGTCAAAAC

Supplementary Table 3. Probes for ChIRP

Probe for	Probe Position	Sequence (5' → 3')
Mouse *Malat1* (NR_002847.2)	142	TTCGATAAGCTACTCTATTAGC
	388	CTTTACTGTTTTAAATGCCACT
	505	AACTCATGCCTTCAAACGTACA
	779	TATCTTCTCTAACAGCTTTTTC
	977	TGACTTTATATCTTATCCAACC
	1192	ATCAAAAGTCCTTTTGTCATCA
	1317	TGTCTTCCTAGTTCACTGAATG
	1710	GTAAACAAGTTACCATCCAAGT
	1903	GTTAAAGACAACTTGCCATCTA
	2031	CAAAAGCACTTTGCCCAATTAC
	2288	GTGTTTAGGATTTTACAAATCT
	2483	CAACTGGGAAAACTCTTCCAAG
	2758	GAGTTACTTGCCAACTTGAAAG
	2933	AATCTATATTCATCCAACAGCT
	3252	CACCCTCTAAAAGACATTCAGG
	3408	TTATTTTTTCTGCCTTTACTTA
	3627	GCTTTTGTAAAAGCAGTTTTGA
	3852	AATACTGCAGATCCAAGTTACA
	4065	TAGGCTTTTGTGTTGAAGTTTA
	4270	CCTTCTAAATACATACATTCTC
	4481	CCTGCAATTATTAAATGCTCAT
	4692	GGCTAAAGTGGATGAGATGATC
	4804	TTATATGCAAAGTCCTGAGCAG
	5072	TTGGGGAAACACAACTTTCTTT
	5316	CAAGAATGTTGCTTGTCTGATT
	5437	CAATGTTCCTGCATGTAAGAAT
	5704	GAGGATTCAACACTAGATTACC
	5919	AATCAAAACCGACCATGATACC
	6122	GATTCTGGAAAAGCTGGGGAAA
	6418	TGGTATCAAACATACTATACCC
	6528	CTGTTATGTCCACCTGAAAAAG
	6729	AAAGACACCGCAGGGACTTGAA
GFP (ORF)	331	TATCACCTTCAAACTTGACTTC
Mouse *U1*	1	CTCCCCTGCCAGGTAAGTAT

SUPPLEMENTARY VIDEOS

Supplementary Video 1. Time-lapse video microscopy of control MDA-MB-231 cells

Supplementary Video 2. Time-lapse video microscopy of *MALAT1* knockout MDA-MB-231 cells

Supplementary Video 3. Time-lapse video microscopy of *MALAT1* knockout MDA-MB-231 cells with ectopic expression of mouse *Malat1*

Supplementary Video 4. Time-lapse video microscopy of control LM2 cells

Supplementary Video 5. Time-lapse video microscopy of *Malat1*-overexpressing LM2 cells

SUPPLEMENTARY NOTE

Supplementary Discussion

***MALAT1* loss specifically affects cancer cells as opposed to normal tissues.** In mice, global *Malat1* knockout does not affect organ growth, development, or primary tumor formation. A possible explanation is that loss of *MALAT1* (and release of endogenous TEAD) is not sufficient to have a functional consequence on its own; instead, it needs to combine with overexpression and/or activation (i.e., nuclear translocation) of YAP. In the mouse models of metastatic breast cancer used in this study, Yap was predominantly localized to the nucleus (Jongchan Kim and Li Ma, unpublished data). Moreover, YAP protein has been reported to be highly enriched in the nucleus of tumor cells from human breast cancer compared with normal mammary tissues[1], which may underlie the specific effect of *MALAT1* loss on cancer cells as opposed to normal tissues. On the other hand, transgenic overexpression of *Yap* in mice promotes organ growth and tumorigenesis[2,3]. A possible explanation is that *MALAT1* and YAP compete with each other for binding to TEAD's transactivation domain; thus, when YAP is overexpressed at a very high level, it may outcompete *MALAT1*. Future studies are warranted to validate these possibilities.

***Malat1* may have dose-dependent effects.** In the genetic rescue experiment, we re-expressed *Malat1* in MMTV-PyMT;*Malat1*$^{-/-}$ mice from a separate locus (*ROSA26*) by crossing these mice to *Malat1*^{Tg} mice to generate MMTV-PyMT;*Malat1*$^{-/-}$;*Malat1*^{Tg} triple mutants. The *Malat1* expression level in MMTV-PyMT;*Malat1*$^{-/-}$;*Malat1*^{Tg} mice was 1.3 fold relative to MMTV-PyMT;*Malat1*$^{+/+}$ mice (**Fig. 1f**; $n = 8$ age-matched mice per group). This was accompanied by slightly less metastasis in MMTV-PyMT;*Malat1*$^{-/-}$;*Malat1*^{Tg} mice compared with PyMT;*Malat1*$^{+/+}$ mice (**Fig. 1b, d, e**). Similarly, we observed a lower percentage of CTCs (**Fig. 1g, h**) and lower mRNA levels of *Itgb4* and *Vegfa* (**Fig. 6b**) in the triple mutants compared with PyMT;*Malat1*$^{+/+}$ mice. In addition, when *Malat1* was overexpressed approximately three times higher either in the transgenic model (**Fig. 2a**) or in the 4T1 syngeneic model (**Supplementary Fig. 5j**), it was sufficient for metastasis suppression (**Fig. 2c-g** and **Fig. 3i, j**). These data indicate that inhibition of Tead activity and metastasis by *Malat1* lncRNA may be dose-dependent.

Supplementary Methods

Generation of targeted *Malat1* transgenic mice. The C57BL/6 mouse embryonic stem (ES) cell line equipped with RMCE docking sites (**Supplementary Fig. 3a**) was grown on a mitotically inactivated feeder layer comprised of mouse embryonic fibroblasts in ES cell culture medium containing leukemia inhibitory factor and fetal bovine serum (FBS). The ES cells were co-transfected with the circular exchange vector containing the transgene and the recombinase pCAG-Flpe pA. From day 2 the medium was replaced daily with medium containing G418. On day 7, resistant ES clones with a distinct morphology were isolated. The clones were expanded and frozen in liquid nitrogen after molecular validation by Southern blotting and PCR. After hormone administration, super-ovulated BALB/c females were mated with BALB/c males. Blastocysts were isolated from the uterus at 3.5 days post coitum, and 10-15 targeted C57BL/6N Tac ES cells were micro-injected into each blastocyst. After recovery, 8 injected blastocysts were transferred to each uterine horn of 2.5 days post coitum, pseudopregnant females. Chimerism was measured by coat color contribution of ES cells to the BALB/c host. Highly chimeric mice were bred to C57BL/6 females. Germline transmission was identified by the presence of black C57BL/6 offspring and confirmed by genotyping. Mice heterozygous for the conditional targeted allele (*Malat1*^{LSL}) were bred to CMV-Cre mice (The Jackson Laboratory, stock #006054) to obtain the constitutive targeted allele (*Malat1*^{Tg}; **Supplementary Fig. 3a**).

Orthotopic model of metastasis and tissue isolation. G418-resistant, luciferase-expressing 4T1 cells (4T1-Luc, $G418^R$) were injected into the mammary fat pad of 6- to 8-week-old female BALB/c mice (n = 10). Mice were monitored by bioluminescent imaging once a week. 7 of 10 mice survived and showed substantial lung metastases. On day 28, mice were euthanized, and paired primary tumors and lungs were dissected, minced, and incubated in a digestive enzyme cocktail containing elastase (6 units/ml, Calbiochem, #324682) and collagenase IV (1 mg/ml, Gibco, #17-104-019) at 4 °C overnight. Next day, tissues were passed through a 70 μm nylon cell strainer (Falcon) and washed with Hanks' buffered salt solution (HBSS) 3 times. Tissues were plated in 4T1 growth medium overnight and then G418 (500 μg/ml) was added to select 4T1-Luc cells. After 2 weeks of selection, cells were harvested for RNA extraction and qPCR analysis.

Animal tissue processing and histopathology. After euthanasia, some tissues were frozen for later RNA and protein extraction, and other tissues were fixed in 10% buffered formalin overnight, washed with PBS, transferred to 70% ethanol, embedded in paraffin, sectioned (5 μm thick), and stained with H&E. Histopathological review was performed on all tissue sections by a pathologist (M. James You). The criteria for histopathological evaluation are as follows: (1) in **Supplementary Fig. 1d**, focal hyperplasia = hyperplasia in 3 or less lobules; hyperplasia = hyperplasia in more than 3 lobules; very small foci of breast adenocarcinoma = breast adenocarcinoma involving 3 or less lobules; small foci of breast adenocarcinoma = breast adenocarcinoma involving 4-6 lobules; breast adenocarcinoma = breast adenocarcinoma involving more than 6 lobules. (2) In **Supplementary Fig. 1e** and **3e**, cystic areas were defined by expanded space lined by double layer of flat/cuboidal cells or no lining, and high-grade tumor areas were defined by malignant epithelial neoplasm with high nuclear/cytoplasmic ratio, mitosis, and prominent nucleoli. (3) The presence of metastasized mammary tumor cells in the lung was based on the presence of primary mammary tumors and at least three cohesive large atypical epithelial cells that had similar morphology as described above (high-grade tumor areas). Digital image pixels of metastatic tumor area (M) and total lung area (L) were quantitated using Photoshop (Adobe), and the percent of lung areas with metastatic lesions was calculated as $100 \times M/L$.

siRNA transfection. Cells were plated in 6-well plates and transfected with 80 pmoles of VEGFA siRNA (Sigma, si-V1, SASI_Hs01_00201117; si-V2, SASI_Hs01_00201118) or a negative control (Sigma, #SIC001) using siRNA transfection reagent (Invitrogen, #13778). After two days, cells were harvested and subjected to invasion assays.

Mass spectrometry. Mass spectrometric analysis was performed according to a previous study[4] with modifications. Proteins pulled down with the ChIRP procedure were eluted in Laemmli buffer and resolved on 4-12% precast NuPAGE gels (ThermoFisher Scientific) to one-fourth length. Gels were stained with Coomassie blue. Gel lanes were sliced into 6 bands and in-gel digested with trypsin at 37 °C overnight. After digestion, peptides were extracted with acetonitrile and dried. Dried peptides were dissolved in a 5% methanol/0.1% formic acid solution. Samples were loaded through a 2 cm C18 trap, followed by 1 hour 4-26% acetonitrile gradient on a 5 cm C18 column, and were analyzed on a Thermo Orbitrap Fusion instrument (Thermo). The raw data were searched with Proteome Discoverer 2.0 Mascot engine against a mouse RefSeq database, and the data were further grouped into gene products that were assigned homology and identification quality groups using an in-house developed algorithm.

Generation of TEAD1 truncation mutants. The N-terminal region (NT) and the C-terminal transactivation domain (TAD) of human TEAD1 (NM_021961.3) were generated using a template plasmid (pPGS-3HA-TEAD1), a mutagenesis kit (QuikChange II XL, Agilent, #200522), and specific primers according to the manufacturer's protocol. Mutagenesis primers are listed in **Supplementary**

Table 2. Vectors containing TEAD1 truncation mutants were treated with the restriction enzyme DpnI to remove the parental plasmid. Sequence-validated TEAD1 truncation mutant constructs were used for transfection.

Immunofluorescent staining. Control and *MALAT1* knockout (KO1) MDA-MB-231 cells were plated in chamber slides (ThermoFisher Scientific, #154917). Next day, subconfluent cells were washed with PBS, fixed, and permeabilized in ice-cold methanol for 7 min. Cells were washed in PBS, blocked in 5% bovine serum albumin, and incubated with a pan-TEAD antibody (1:100, Cell Signaling Technology, #13295) at 4 °C overnight, followed by incubation with Alexa Fluor 488 goat anti-rabbit IgG (1:500, ThermoFisher Scientific, #A11008). Slides were then washed and mounted with VECTASHIELD Antifade Mounting Medium with DAPI (Vector laboratories, #H-1200).

Nuclear and cytoplasmic extraction. Control and *MALAT1* knockout MDA-MB-231 cells were plated in 15 cm dishes. Fractionation of nuclear and cytoplasmic proteins was done by using the NE-PER Nuclear and Cytoplasmic Extraction Kit (ThermoFisher Scientific, #78833) according to the manufacturer's protocol. After protein extraction, Western blot analysis was performed to detect TEAD proteins in cytoplasmic and nuclear fractions. α-tubulin and Lamin B1 were used as markers of the cytoplasm and the nucleus, respectively.

Immunoprecipitation. HEK293FT cells were transfected with pPGS-3HA-TEAD1, SFB-YAP, and/or pcDNA3.1(-)-*Malat1* and harvested 2 days post transfection. Cells were lysed in NETN buffer (20 mM Tris-HCl at pH 8.0, 100 mM NaCl, 1 mM EDTA, 0.5% NP-40). SFB-YAP and HA-TEAD1 were immunoprecipitated with S-protein agarose (Novagen, #69704) and HA antibody-conjugated agarose beads (Sigma, #A2095), respectively. SFB: a triple-epitope tag containing S-protein, FLAG, and streptavidin-binding peptide.

Cell proliferation assay. 1,000 LM2 and 2,000 MDA-MB-231 cells were seeded in 96-well plates and incubated. Next day (day 1), one plate was taken from the incubator, and each well was washed once with PBS, followed by staining of cells with 0.2% crystal violet in 10% formalin. Excessive stain was washed with tap water and plates were air-dried. The procedure was repeated on day 2, 3, and 4. Stained cells were de-stained with 50 μl of 10% acetic acid and the optical density was measured at 570 nm on a Gen5 Microplate Reader (BioTek).

Soft agar assay. Soft agar assays to examine anchorage-independent growth was performed as previously described[5]. Briefly, 2,000 cells were mixed with 0.35% soft agar in 1× growth medium and plated in 6-well plates on the top of 0.5% soft agar in 1× growth medium. After 6 weeks, colonies were photographed and counted.

Migration and invasion assays. Cell migration (Corning, #3422) and invasion (Corning, #354480) were gauged using Boyden Chambers. 1×10^4 and 2.5×10^4 LM2 cells, 2×10^4 and 5×10^4 MDA-MB-231 cells, and 3×10^4 and 6×10^4 HCC1806, BT549, Hs578t, and SUM149 cells were re-suspended in serum-free and growth factor-free medium and added to the upper chamber for migration and invasion assays, respectively. To examine whether VEGFA promotes invasion, we added 20 ng/ml of recombinant human $VEGFA_{165}$ (R&D Systems, #293-VE-010) or bovine serum albumin as a control protein to the upper chamber, as previously described[6]. Serum-containing growth medium was added to the bottom chamber. 20-24 hours later, cells on the upper surface of the membrane were removed with a cotton swab, and cells on the lower surface of the membrane were stained with 0.2% crystal violet, photographed, and counted.

Time-lapse video microscopy. 12-well plates were coated with 0.5 ml of 1.7 mg/ml collagen I solution (VWR, #354231). After collagen solidified, cells were plated in complete growth medium on top of the collagen and were incubated overnight. Next day, cells were washed in PBS, and serum-free and growth factor-free medium was added to minimize cell proliferation. Random cell movement was captured every 30 minutes for 24 hours in a humidified, CO2-equilibrated chamber mounted on a Zeiss Axio Observer Z1 microscope. Video files were generated and analyzed by Imaris image analysis software to track the distance of individual cell movement and to quantitate the speed in randomly selected fields. The speed of movement was presented as nanometers per second.

RNA splicing pattern analysis. For RNA splicing pattern analysis, paired-end raw sequencing reads were mapped to the mouse reference genome (mm10) using OLego[7] with default parameters. This step mapped reads to exons, known junctions, and novel junctions. We required at least 5 nucleotides match on either side of the junction for known junctions, and more than 8 nucleotides overlap for novel junctions. The maximum number of mismatches allowed for each read was determined by the read length. We then inferred splicing isoform structure using Quantas gapless through a Bayes model (see URLs). After that, the expression level of each isoform was calculated and compared between *Malat1* wild-type and knockout groups to identify significant splicing changes using Quantas countit (see URLs). We pooled the reads count together from biological replicates and performed Fisher's exact test using the total number of supporting reads of each isoform in different groups on ~16,000 annotated cassette exons. Statistically significant changes were defined using the cutoff values recommended by the software used: false discovery rate, FDR < 0.01, and proportional change of inclusion level, $|\Delta I| > 0.2$.

Tumor metastasis PCR array. The 96-well format Tumor Metastasis RT^2 Profiler PCR Array (Qiagen, #PAHS-028Z), consisting of 84 genes known to be involved in metastasis, was used to profile *Malat1*-overexpressing LM2 cells. Total RNA was extracted from control and *Malat1*-overexpressing LM2 cells using the RNeasy Mini Kit (Qiagen) and DNase I treatment. Reverse transcription and qPCR were performed according to the manufacturer's protocol. Briefly, after reverse transcription, the cDNA was combined with an RT^2 SYBR Green qPCR Master Mix (Qiagen), and then equal aliquots of this mixture were added to each well of the PCR Array plate that contains the pre-dispensed gene-specific primer sets. Real-time PCR and data collection were performed on a CFX96 instrument (Bio-Rad). Genes that had a Ct value < 35 (63 of 84 genes) and showed >50% downregulation in *Malat1*-overexpressing LM2 cells relative to control LM2 cells were selected for further analysis.

Reporter assays. 8× GTIIC firefly luciferase and *VEGFA*-luciferase (V1: -500 to -1; V2: -1000 to -1) vectors were from Addgene (plasmid numbers: #34615, #66130, and #66128). For reporter assays of firefly luciferase-labeled cells, 8× GTIIC TEAD-binding sequences were cloned from the 8× GTIIC firefly luciferase vector to the NanoLuc luciferase vector (Promega, #N1071). The pG5-luc vector was from Promega (#E2440). Full-length human YAP (aa 2-504) and the transactivation domain (aa 291-504) were cloned into the pBIND vector (Promega, #E2440) with restriction enzymes XbaI and NotI to make GAL4 DNA binding domain (DBD)-fused YAP constructs. *ITGB4*-luciferase vectors (L5.5, L2, L3, L6, L7, L8, L9, and L10) were from Jeffrey Jacobson (University of Illinois at Chicago). HEK293FT cells were plated in triplicate in 96-well plates with white polystyrene upper structure (Nunc). Next day, 16.67 ng of the indicated luciferase vectors, 0.1 ng of a Renilla luciferase vector, 50 ng of SFB-YAP, 50 ng of pPGS-3HA-TEAD1, and 20 ng or 100 ng of pcDNA3.1(-)-*Malat1* were transfected per well. For luciferase assays with GAL4 DBD-fused proteins, 10 ng of pG5-luc, 1 ng of a Renilla luciferase vector, 50 ng of pBIND (GAL4 DBD only), GAL4-TAD, or GAL4-FL, and 10 ng or 50 ng of pcDNA3.1(-)-*Malat1* were transfected per well. 2 days post transfection, firefly and Renilla luciferase activities were measured using a Dual-Luciferase Reporter Assay system (Promega, #E1910) on a Gen5 Microplate Reader (BioTek) according to the manufacturer's protocol. Firefly luciferase activity was normalized to Renilla luciferase

activity. For NanoLuc luciferase assays with firefly luciferase-labeled MDA-MB-231 cells (control and *MALAT1* knockout clones), 70,000 cells were plated in triplicate in 24-well plates. 0.25 μg of the β-galactosidase vector (Promega, #E1081), the empty NanoLuc vector, 8× GTIIC-NanoLuc, and SFB-YAP were transfected per well. 2 days post-transfection, cells were washed with PBS and 200 μl of passive lysis buffer (Promega, #E1941) was added to each well. 50 μl of lysate from each well was added to opaque-wall and clear-wall 96-well plates, and NanoLuc luciferase activity and β-galactosidase enzyme activity were measured using the Nano-Glo Dual-Luciferase Reporter Assay System (Promega, #N1610) and the β-Galactosidase Enzyme Assay System (Promega, #E2000), respectively, according to the manufacturer's protocol. NanoLuc luciferase activity was normalized to β-galactosidase enzyme activity.

Enzyme-linked immunosorbent assay (ELISA). 4×10^5 cells were plated in 6-well plates. Next day, cells were washed with PBS and 700 μl serum-free growth medium was added. After 48 hours, conditioned media were harvested, centrifuged to remove cell debris, and diluted to 1/10 for ELISA using a VEGF assay kit (VWR, #EK0539) according to the manufacturer's protocol.

Supplementary References

1. Steinhardt, A.A. *et al.* Expression of Yes-associated protein in common solid tumors. *Hum Pathol* **39**, 1582-9 (2008).
2. Dong, J. *et al.* Elucidation of a universal size-control mechanism in Drosophila and mammals. *Cell* **130**, 1120-33 (2007).
3. Camargo, F.D. *et al.* YAP1 increases organ size and expands undifferentiated progenitor cells. *Curr Biol* **17**, 2054-60 (2007).
4. Malovannaya, A. *et al.* Analysis of the human endogenous coregulator complexome. *Cell* **145**, 787-99 (2011).
5. Kim, J., Roh, M. & Abdulkadir, S.A. Pim1 promotes human prostate cancer cell tumorigenicity and c-MYC transcriptional activity. *BMC Cancer* **10**, 248 (2010).
6. Luo, M. *et al.* VEGF/NRP-1axis promotes progression of breast cancer via enhancement of epithelial-mesenchymal transition and activation of NF-kappaB and beta-catenin. *Cancer Lett* **373**, 1-11 (2016).
7. Wu, J., Anczukow, O., Krainer, A.R., Zhang, M.Q. & Zhang, C. OLego: fast and sensitive mapping of spliced mRNA-Seq reads using small seeds. *Nucleic Acids Res* **41**, 5149-63 (2013).